BIOMECHANICAL PROPERTIES OF ANTERIOR VAGINAL WALL TISSUE IN POST-MENOPAUSAL WOMEN

by

ARADHANA BHATT

Presented to the Faculty of the Graduate School of

The University of Texas at Arlington in Partial Fulfillment

of the Requirements

for the Degree of

MASTER OF SCIENCE IN BIOMEDICAL ENGINEERING

THE UNIVERSITY OF TEXAS AT ARLINGTON

August 2005

ACKNOWLEDGEMENTS

I would like to express my sincere gratitude to the all members on my thesis committee for their help and support they have extended through the course of my project. I would like to thank Dr Eberhart and Dr Zimmern for giving me the opportunity to work on this project, for their constant guidance, motivation and encouragement. It has been my great pleasure. I would also like to thank David Muirhead for allowing me to work in the lab after hours and for all the guidance, support and motivation in putting this thesis together. I wish to thank Dr Chuong for his advice and support.

I would also like to thank Devraj Subramaniam, Dwight Bronson and Bill Rademaker for their help with the mechanical testing. I would like to thank the research group Dr. Victor Lin and Dolores Vazquez. This project was supported by an internal grant from the Department of Urology and I would like to thank Dr Claus Roehrborn.

I would also like to express my sincere gratitude to the BME program faculty for the opportunity to be a part of the program.

I would like to thank my parents for their love and support. I would also like to thank all my friends for their words of encouragement and for all their help. Thank you Tre′ for recovering my document.

July 21, 2005

ABSTRACT

BIOMECHANICAL PROPERTIES OF ANTERIOR VAGINAL WALL TISSUE IN POST-MENOPAUSAL WOMEN

Publication No. _____

Aradhana Bhatt, MS (BME)

The University of Texas at Arlington, 2005

Supervising Professor: Robert C. Eberhart

Cystocele repair in post-menopausal women suffering from urinary incontinence and associated vaginal prolapse is a common method of palliation. In this method, there is surgical reduction of vaginal tissue and the weak cross-sections are often supported with a synthetic sling fashioned from polymer mesh material. Some sling-supported and unsupported repairs fail over the years. The reasons for these failures are unclear, due in part to a lack of fundamental knowledge of the mechanisms associated with cystocele and vaginal prolapse. The aim of this study was to understand the mechanisms of tissue failure by biomechanical and ultrastructural studies. We take advantage of the availability of fresh samples of excised vaginal tissue taken from

postmenopausal women undergoing cystocele repair. Control samples were obtained from patient without cystocele and vaginal prolapse. Samples were stored at room temperature for less than two hours prior to analysis, either in unbalanced saline solution (Group 1), or as placed on saline-moistened gauze (Group 2). Mechanical property measurements under uniaxial tension, histological analysis and histomorphometrical measurements were performed on Group 1, 2 and control samples. Based on the broad set of measurements and associated analyses, it was possible to discern differences in mechanical and ultrastructural properties associated with hydration during storage, and with the disease process. The group 1 tissues were found to be weaker than the group 2 tissues. Stretching of the tissues caused the collagen fiber diameter to decrease and the fiber periodicity to increase. On measuring the thickness of the epithelium there was a significant difference between an unstretched and stretched prolapse tissue. Although the control sample population was insufficient for comparative analysis, the results suggested links may exist between the mechanical and ultrastructural properties of prolapsed and unprolapsed tissues. With further examination we aim to design and implement improved palliation procedures.

TABLE OF CONTENTS

Appendix

LIST OF ILLUSTRATIONS

LIST OF TABLES

CHAPTER 1

INTRODUCTION

1.1 Background

Prolapse comes from the Latin word, "to fall." In medicine, this term indicates that an organ has slipped out of its proper place. There are several kinds of prolapse relevant to urology and gynecology. Women with pelvic floor disorders may suffer from the rectum protruding through the back wall of the vagina (rectocele), the bladder protruding out through the anterior vaginal wall (cystocele) or the entire vagina (vaginal vault prolapse) or uterus (uterine prolapse) prolapsing through the vaginal opening. The small intestine may even prolapse (enterocele), especially in women who have had a hysterectomy. When an organ presents through a vaginal prolapse, it may be indicative of an unusually difficult labor during childbirth, multiple childbirths, obesity or the effects of constant straining on the female pelvic floor. Symptoms of urinary incontinence, rectal and/or vaginal heaviness and pain, constipation, and discomfort or pain experienced during sexual activity, may indicate vaginal prolapse.

The annual direct costs of operations for pelvic organ prolapse are substantial. According to a study conducted in 1997 by Subak et al., direct costs of pelvic organ prolapse surgery was $1012 million of which $279 million constituting 28% of the total cost was for cystocele and rectocele repair. Physician services accounted for 29% ($298 million) of total costs, and hospitalization accounted for 71% ($714 million).

Twenty one percent of pelvic organ prolapse operations included urinary incontinence procedures ($218 million). If all operations were reimbursed by non-Medicare sources the annual estimated cost would increase by 52% to $1543 million [1].

Anterior vaginal prolapse results from direct or indirect damage to the pelvic muscles and connective tissue or both. Vaginal reconstructive surgery for pelvic organ prolapse is one of the most challenging aspects of surgical urology and gynecology, and recurrence is particularly troublesome in the anterior vagina. Failure rates of 0- 20% were reported for anterior colporrhaphy and 3-14% for paravaginal repair [2].

Subak et al reported the currently available estimates to 225,000 inpatient surgical procedures for prolapse performed every year in the United States. The estimated direct medical costs are over one million dollars [3]. The number of cases and the associated cost along with the complications that followed prompted this fundamental study of the anterior vaginal wall prolapse.

1.2 Anatomy of the anterior vagina

The vagina is a fibromuscular tube, which extends from the vestibule to the cervix. Histologic examination of the vagina demonstrates three layers – mucosa, muscularis, and adeventitia. The mucosa is a non-keratinizing squamous epithelium overlying a thin, loose connective tissue layer, the lamina propria. The muscular layer consists primarily of smooth muscle, with smaller amounts of collagen and elastin. The adventitial layer is a variably discrete connective-tissue layer of collagen and elastin between the muscular wall of the vagina and the adjacent paravaginal connective tissue [2, 4]. Normal anatomy of the adult vagina is shown in Figure 1.

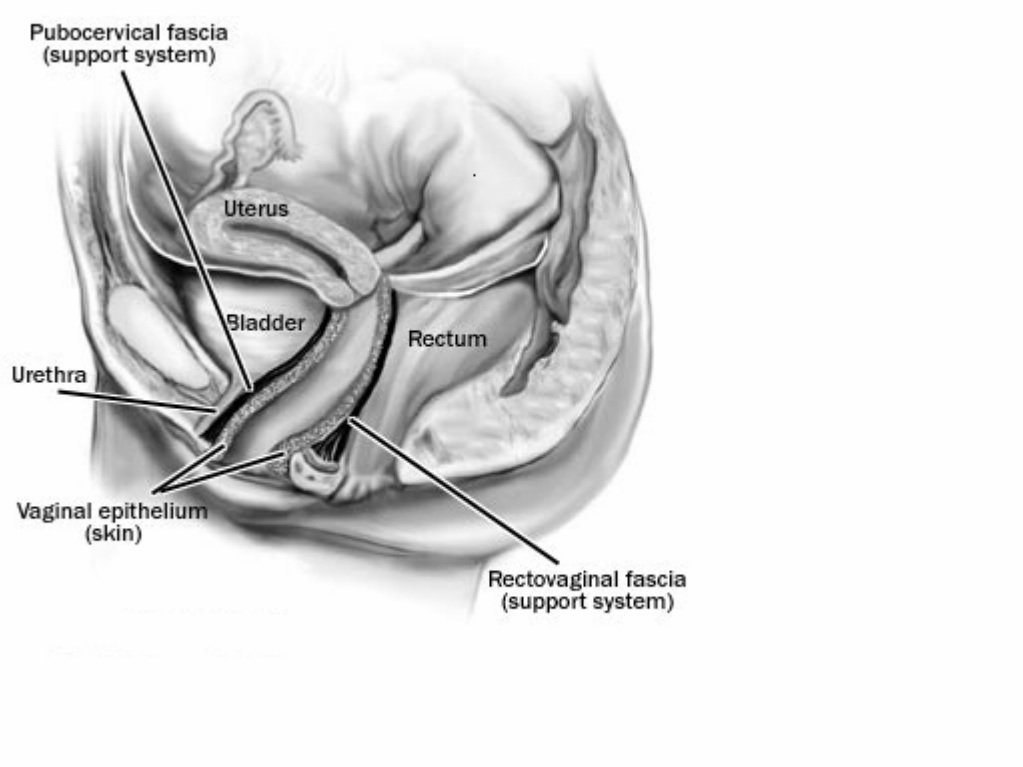

Figure 1 Normal adult vaginal anatomy.
(Source: http://www.obgyn.net/)

1.3 Support of the anterior vagina

Support of the vagina is provided by interaction between the pelvic floor muscles (levator ani) and connective tissue. In the absence of prolapse, the upper two-thirds of the vagina lies nearly horizontal, supported by the underlying levator muscles. The lateral aspects of the anterior vagina are attached on each side by fibrous connections to the parietal fascia over the levator, forming the "white line" or arcus tendineus fasciae pelvis that extends from the pubic symphysis to each ischial spine. These fibrous connections stabilize the vagina over the levator muscles, which normally contract continuously. This combination provides effective support against the intra-abdominal pressure forces.

The bladder, without distinct supports of its own, is maintained in position by resting on the anterior vagina. The urethra is supported not only by the anterior vagina but also by the perineal membrane and its muscular components, the urethrovaginal sphincter and compressor urethrae [2].

1.4 Causes of prolapse

Some researchers suggest that in some women the damage incurred during vaginal birth predisposes to the development of prolapse, but there is less agreement on the nature of the damage. Some authors describe stretching of the vaginal tissue beyond its capacity to recover, with thinning of the vagina, exacerbated by aging and estrogen deficiency of menopause, which corresponds to the "distension" type of cystocele. This type of cystocele can be distinguished by the loss of vaginal rugal folds [2].

Other factors that may contribute to the development of prolapse include abnormalities in collagen biosynthesis with the resultant weakness of connective tissue and the damage to pudendal nerves that occurs during vaginal birth, resulting in abnormal functioning of the levator muscles. When the levator muscles are damaged or otherwise function poorly, the fibrous connections are exposed, unprotected from the downward intra-abdominal pressure forces. Unable to withstand chronic tension, the fibrous connections may then elongate or break, resulting in prolapse [2].

The biomechanics of the vaginal wall have not been thoroughly studied nor is there ultrastructural evidence to support the cited causes. Figure 2 shows the vaginal herniation.

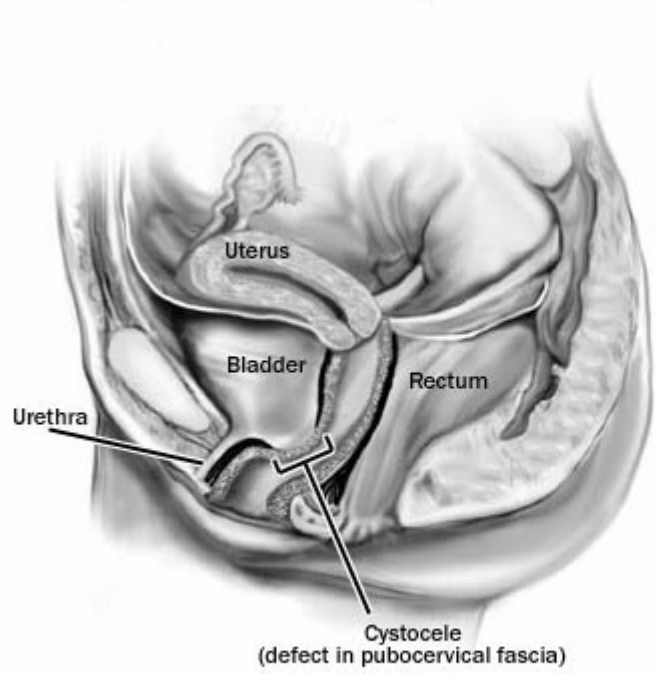

Figure 2 Cystocele.
(Source: http://www.obgyn.net/)

1.5 Repair of anterior vaginal wall prolapse

Anterior colporrhaphy has been the standard surgical treatment for anterior vaginal prolapse [5]. Anterior repair is a vaginal procedure designed to "tack" or suture the bladder into its normal anatomic position. It is often used to correct a cystocele and to manage stress urinary incontinence. This surgery is particularly helpful when the cystocele is caused by a defect in the midline support tissue between the bladder and vagina. The procedure illustrated in Figures 3 and 4, begins with dissection of the overlying vaginal epithelium from the underlying pubocervical fascia. The defect in the pubocervical fascia is identified and repaired using sutures. The excess vaginal skin is

removed in order to give the vagina more strength. Often the skin stretches and only the excess should be removed. Finally the vaginal skin is closed using suture. Through a vaginal incision, the bladder is returned to its position behind the pubic bone. Often synthetic meshes are placed to support the vaginal wall and to keep the prolapsed organ in place.

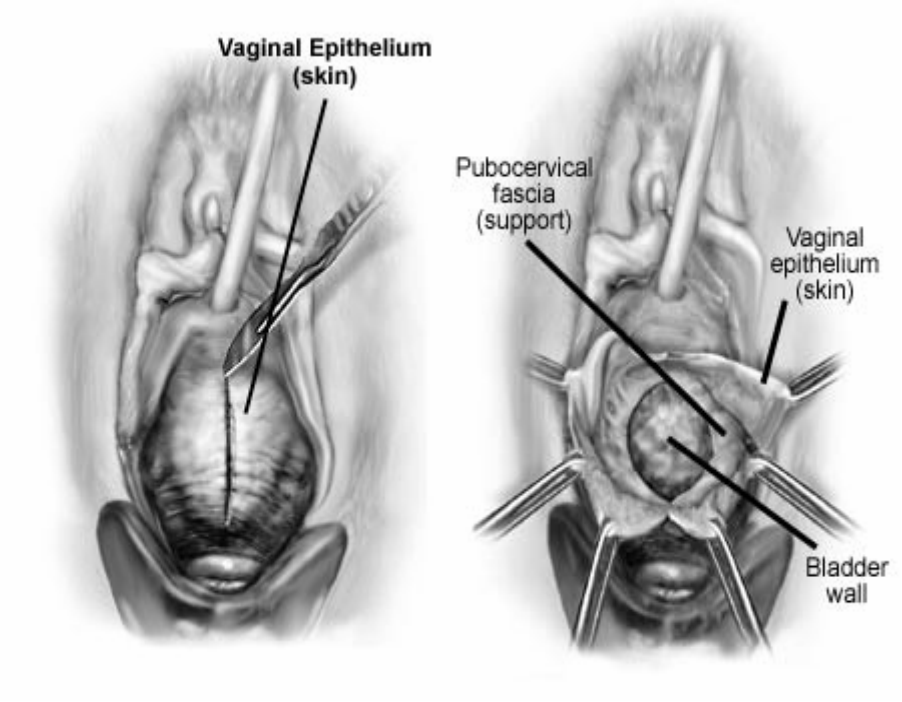

Figure 3 (a) An incision is made on the epithelium, (b) Identification of midline defect. (Source:http://www.obgyn.net/)

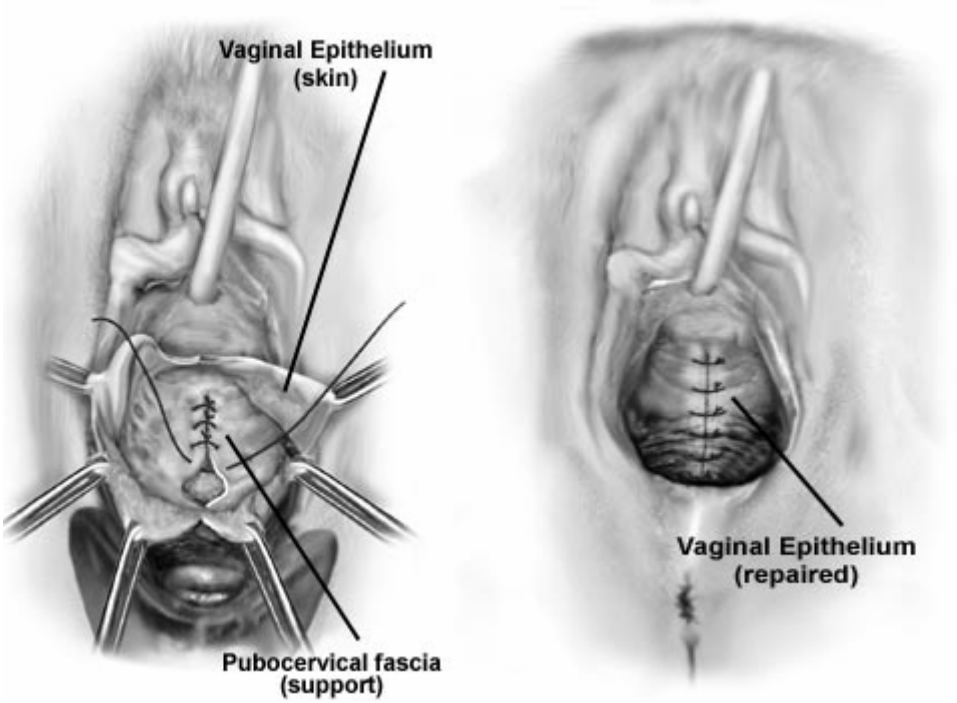

Figure 4 (a) Excess skin is removed and sutures are placed repairing the defect. (b) vaginal epithelium is repaired and closed.(Source: http://www.obgyn.net/)

1.6 Support systems for the vagina

Synthetic and autologous materials have been widely used in the field of urology and urogynecological surgery to provide additional support for the repaired organ. The advantages and disadvantages of synthetic and autologous materials are described in Table 1[6].

Table 1 Advantages and disadvantages of synthetic meshes over autologous donor grafts.

	Synthetic meshes	Autologous donor grafts
Advantages	a) ready availability b) lower cost c) consistent strength and predictable tissue response	a) in vivo tissue remodeling b) histologic similarity to native vaginal wall tissue c) reduced incidence of erosion
Disadvantages	a) failure of remodeling b) limited stretch properties c) potential of inflammation, infection and erosion.	a) limited supply with increased cost b) inconsistency of tissue strength c) lack of long term outcome data

Synthetic meshes are extensively used in hernia repairs. The types of meshes vary substantially with regard to the composition of the fibers, type of weave, pore size, tensile strength and flexibility of the material. Synthetic materials such as polyethylene terephthalate, expanded polytetrafluoroethylene (ePTFE or Gore-tex), polypropylene mesh (prolene) have been used as meshes in gynecological surgeries. The use of these synthetic materials has been associated with varying degrees of localized tissue reaction, infection and urethral erosion. They are not very popular and are not used to a great extent. Pore size and mesh weight are considered key factors in determining the

inflammatory response and growth of fibrocollageneous tissue. Macroporous mesh is thought to allow rapid ingrowth of vascularized fibrous tissue. This causes fibroplasia and angiogenesis which is said to prevent infection and form fibrous connections to the surrounding tissue. Smaller pore sizes may be inadequate as they may inhibit or prevent capillary penetration [7].

The autologous donor grafts including, cadaveric fascia, human and porcine dermis and small intestine submucosa have been used in reconstructive pelvic surgery. The tensile strength, antigenicity and inadequate tissue remodeling are suboptimal. The critical properties of these tissues remain to be determined. In addition viral infections with use of autologous donor grafts pose a potential concern [6].

1.7 Scope of work

Vaginal prolapse and urinary incontinence degrade the quality of life, but are not life threatening. Nevertheless, for the elderly patient, these are major problems that seriously destabilize the patient's equilibrium and detract from the sense of well being. Perhaps because they are not life threatening, very little work has been done to categorize the failure of the vaginal tissue, to quantify the tissue characteristics of young patients with normal vaginal tissue, to understand the mechanisms of tissue failure as it relates to organ dysfunction. Various studies have been conducted to study the kinds of collagen present in the tissue, effect of hormonal therapy, changes in hormones brought about by menopause, collagen alteration in patients with prolapse, effect of aging and number of child births, child delivery through the vaginal canal, and collagen composition in the levator ani muscles. The effect of various surgical methodologies

for anterior vaginal wall repair has been explored. In all these studies an attempt to understand the inherent nature of the anterior vaginal wall was not addressed. Knowledge of the anatomy and structural details, with precise identification of the modes of failure of the prolapsed vaginal wall tissue, will aid in the understanding of the nature of the problem. An optimal support for the reconstructed tissue can then be designed. It will also aid in the design of a mesh-based sling that is specifically adapted to vaginal support to replace the general-purpose slings currently employed.

Thus the principal aims of this research were to:

1) Quantify the mechanical properties of the excised portions of the prolapsed vaginal wall vs. age-matched controls;

2) Measure the mass and organization of collagen and other substances within the tissue;

3) Attempt to correlate the collagen properties with the mechanical properties.

1.8 Rationale of the study plan

The main aim of this study was to document biomechanical and ultrastructural properties of the excised prolapsed tissue as is and following uniaxial stressing to tissue failure. This will assist in determining the causes of tissue failure in the case of anterior vaginal wall prolapse. The mechanical properties of the tissue would assist in determining nature of the tissue failure. A comparison of mechanical properties between a healthy control tissue and a prolapse tissue would be effective in determination of differences between the two. With an improved understanding of the mechanical properties of the tissues, a qualitative and quantitative examination of the

ultrastructure of the tissue would be key in determining the pathology of this disease condition. It can be hypothesized that: 1) the control tissue is mechanically stronger than the prolapsed tissue, and 2) the control tissue ultrastructure exhibits normal distribution and arrangement of the collagen fibers, adequately support the tissue, incontrast to the prolapse samples. The bioengineering rationale for these studies is that a more effective support system for each patient may be designed, one that depends on the degree of prolapse. However in the study outlined here, emphasis is laid in understanding the nature of the prolapsed anterior vaginal wall tissue itself. The future of the project would be to design a mesh that would mimic the healthy tissue or a drug-eluting mesh that could promote healing of the damaged tissue.

1.9 Study outline

This study was based on research conducted by Chuong et al. on the anisotropy of the canine diaphragm, where the mechanical properties of the central tendon were studied. Uniaxial stress-strain test were performed. Histological sections were prepared to examine the collagen-layered structure [8]. The outline of the biomechanical study was to determine the biomechanical properties of anterior vaginal wall (Figure 5).

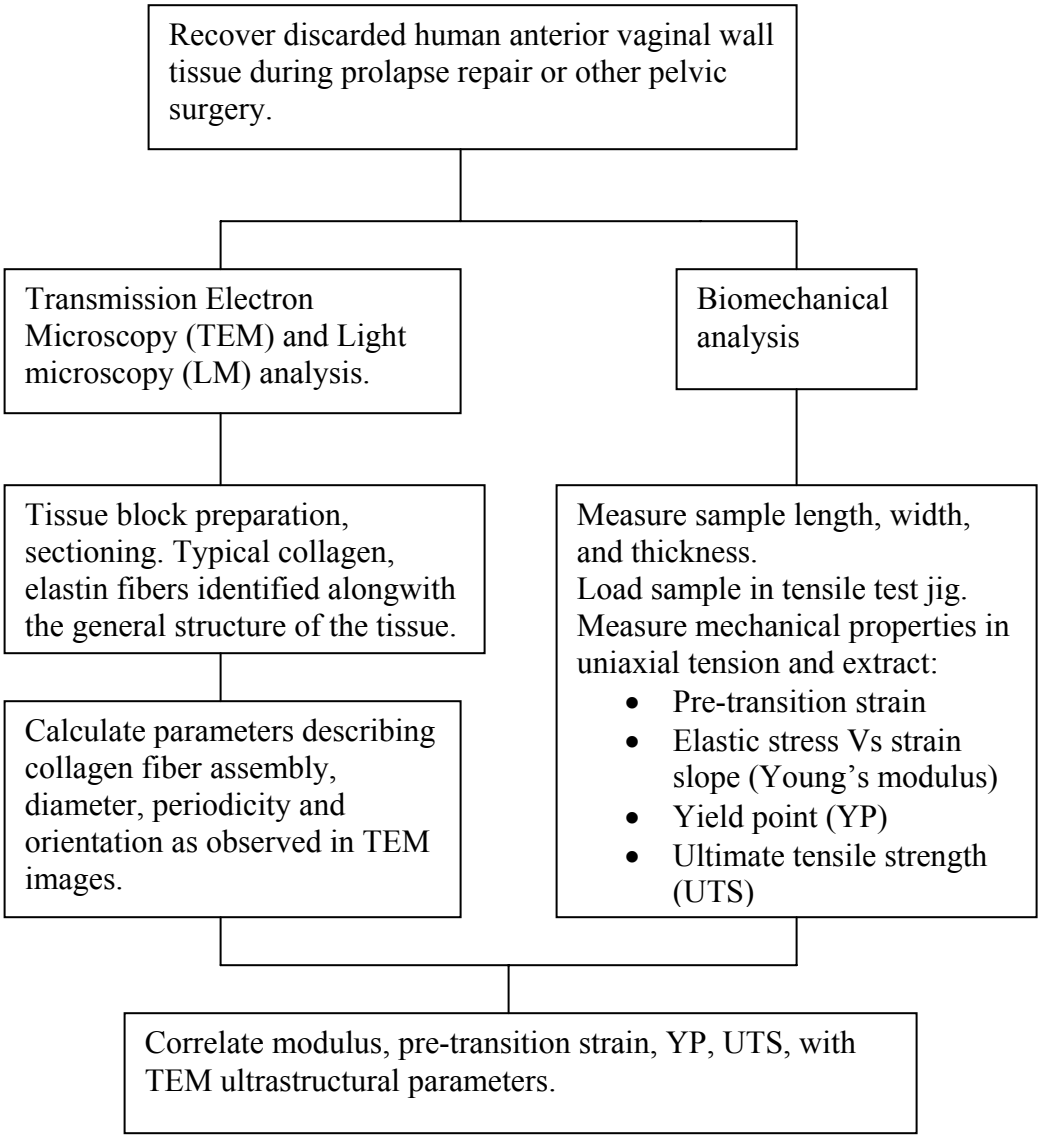

Figure 5 Outline of the study.

CHAPTER 2

MATERIALS AND METHODS

The research was performed to investigate the mechanical properties and tissue structure of specimens harvested from females undergoing surgical treatment for anterior wall vaginal prolapse. This chapter describes the methods used to characterize the mechanical, histological, and ultrastructural properties of the anterior vaginal wall. Consent was obtained from female patients participating in this IRB-approved study. In addition to samples obtained from patients with stage III sand IV vaginal prolapse, control samples were acquired from asymptomatic females with no evidence of prolapse disease, who underwent other urological and gynecological surgical procedure.

Mechanical testing was conducted on all the tissue samples. They were subjected to uniaxial tension, employing a standard materials testing system Bionix 858(MTS corporation, Minneapolis, MN, USA), designed to evaluate both synthetic and biomaterials for yield and ultimate strength, creep and viscoelastic characteristics, fatigue characteristics, elasticity and other biomechanical properties. Such systems are widely used whenever the mechanical characterization of implant materials is of importance. In this study the use was limited to stretching of samples at a steady rate until tissue failure. All generated data of load and displacement was recorded electronically.

Tissue structure was analyzed by light microscopy (LM), transmission electron microscopy (TEM) and basic histomorphometry. Light microscopy permitted morphological and histological assessment of the gross structure of the anterior vaginal wall after tissue failure due to tensile loading. TEM enabled the assessment, at high magnification (x12390), of collagen fiber bundle size, orientation and periodicity.

2.1 Sample collection and preparation

Tissue samples were harvested as part of an anterior vaginal wall suspension procedure typically used to correct a Stage III or IV anterior vaginal wall herniation known as cystocele. In this condition the bladder bulges into the vagina due to weakening of certain tissue (fascia) between the anterior vagina and the bladder. Most females that have cystocele sense a bulge into the vagina, as shown in Figure 6. Cystocele repair is a relatively simple surgical procedure to repair the fascia surrounding the vagina, to restore the normal anatomy. A synthetic fiber mesh, such as prolene is often stapled to the fascia to reinforce the structure.

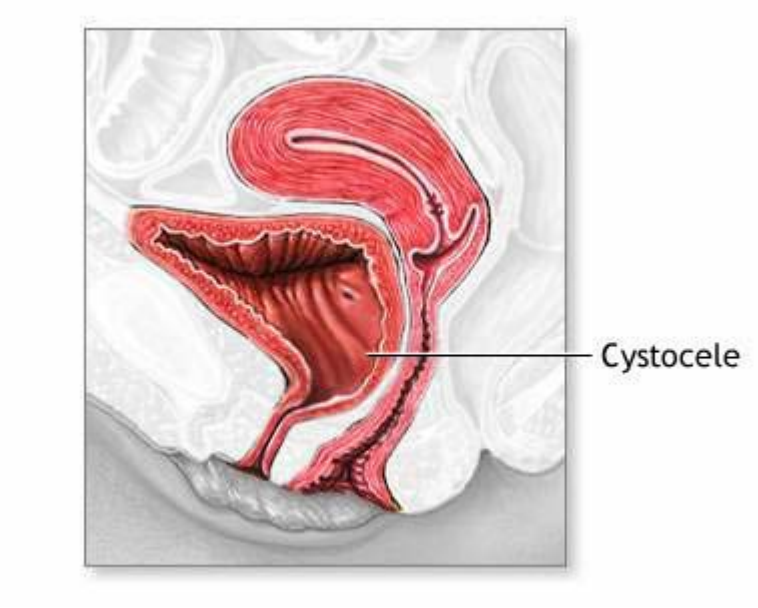

Figure 6 A Cystocele showing the bladder drooping into the vagina.
(Source: http://www.nlm.nih.gov/medlineplus/ency/imagepages/9064.htm)

IRB approval (Appendix A) was obtained for the use of the excised vaginal wall tissue. Anterior vaginal wall strips lateral to the midline vaginal plate and corresponding to the site of the lateral defect was excised. The lateral extent is terminated approximately 5-10 mm from the lateral vaginal wall sulcus, which is left intact. The samples were excised from the bladder neck, level to the vaginal apex, either unilaterally or bilaterally depending on the extent of the cystocele (Figures 7, 8, 9, 10). Samples were also obtained from asymptomatic females who underwent radical cystectomy.

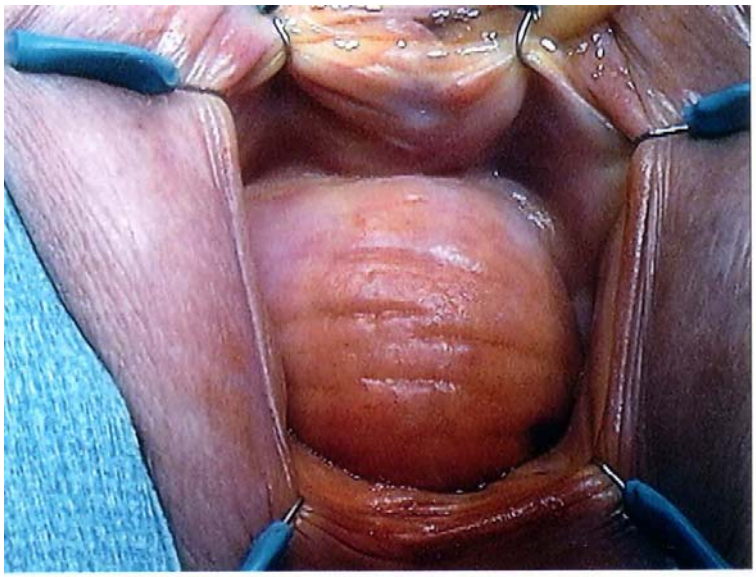

Figure 7 The bladder hernia (cystocele) is seen as a bulge in the opening of the vagina

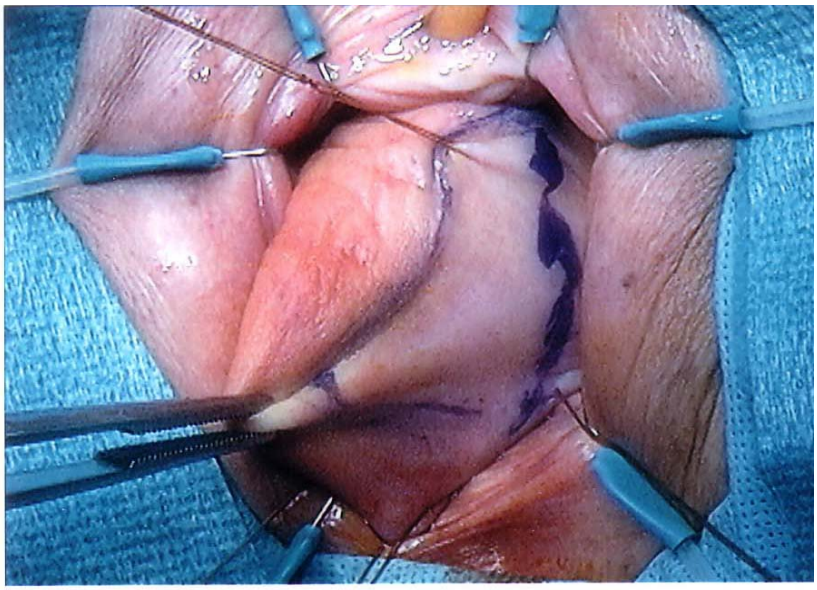

Figure 8 The tissue to be excised is marked and prepared for excision

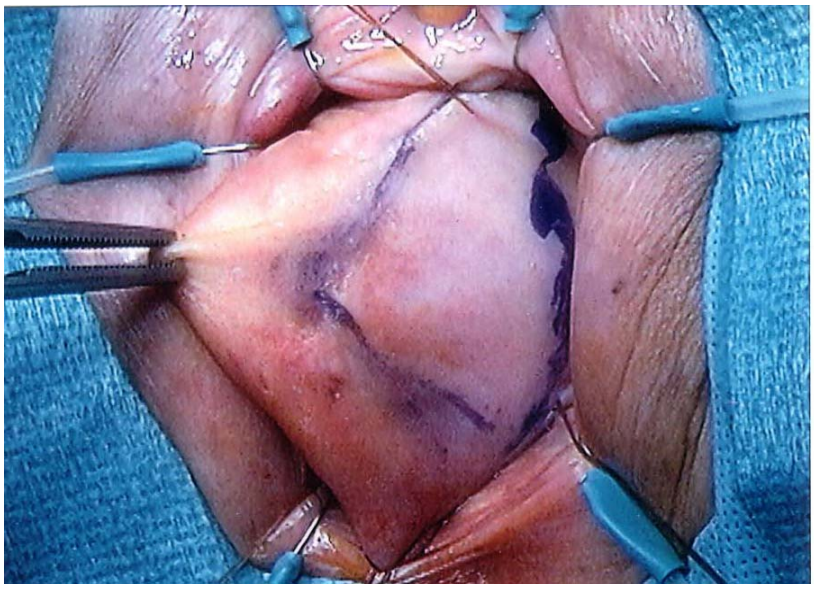

Figure 9 The tissue to be excised is identified, marked and a suture is placed on the top part of the tissue for excision

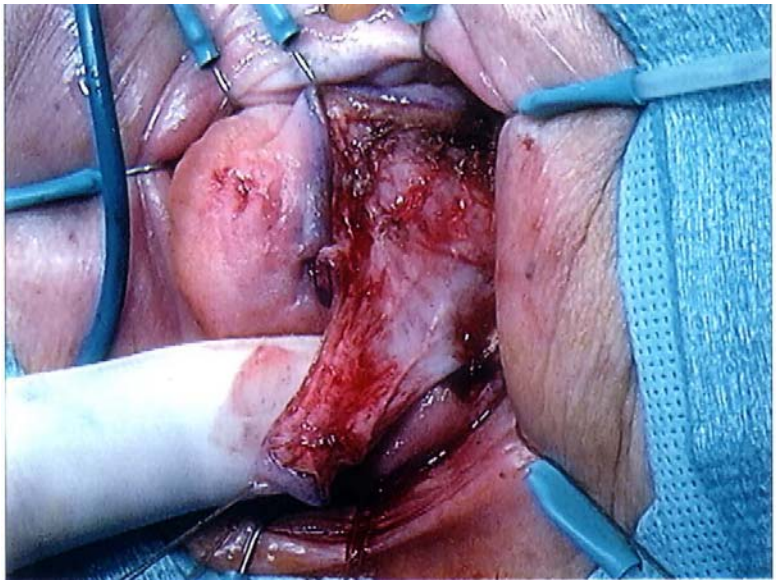

Figure 10 The marked tissue is excised and sent for analysis

Where possible, two samples of anterior vaginal wall tissue were obtained from each patient. All samples were harvested with the same orientation so as to maintain consistency. A suture placed at the distal extremity of the specimen, prevented mechanical tissue damage artifact during harvest, and provided an orientation marker for biomechanical studies. Cauterization, indentation or small side cuts in the strip edges, which could promote tearing during the biomechanical studies, were prevented. All samples had a minimum width of 1 cm and had consistent length of approximately 3 cm. (See Figure 11). When cystocele was pronounced, another piece of tissue was harvested for the TEM analysis measuring approximately 1x1x0.5 cm.

Figure 11 Excised tissue sample of the anterior vaginal wall

The harvested tissue samples were prepared for transport to the biomechanics laboratory. In the initial stages of the study the tissue samples were immersed in saline; in the latter part of the study, tissue samples were wrapped in gauze moistened with a

few drops of saline. A mechanical test was conducted on two tissue samples obtained from a prolapse patient to investigate the effect of the two modes of transport, which were adopted during the course of this study. Sixteen samples were identified to having been immersed in saline and the twenty-three samples were wrapped in gauze moistened with a few drops of saline. They were closely analyzed for the effects of hydration on tissue properties. Three control samples were obtained which were subjected to the second mode of transport. The mechanical test was performed on the tissue samples within two hours of tissue harvest to minimize its mechanical deterioration.

2.2 Mechanical testing of the harvested tissue sample

Mechanical properties of the harvested sample are indicative of the strength or weakness of the tissue and provide important information on the tissue characteristics. An understanding of these properties is of great importance from the perspective of developing a realistic framework; particularly the effect that microstructural modifications from aging, disease, remodeling, etc., can have in degrading the tissue. A protocol for testing the mechanical properties of the tissue was designed. The harvested samples were subjected to uniaxial tensile load and the corresponding load and displacement was measured. The behavior of the tissue under the loaded condition, Young's modulus (E), ultimate tensile stress (UTS) and the point at which the tissue ruptures or the yield point (YP) are important parameters in determining the properties of a tissue.

2.2.1Uniaxial tension measurements

Testing was performed using a material testing machine (MTS Bionix 858, Minneapolis, MN) designed to test the tissue for yield and ultimate strength, creep and viscoelastic characteristics, fatigue characteristics, elasticity and other biomechanical properties. The machine was used to obtain the load displacement characteristics of the anterior vaginal wall tissue. The accuracy of the MKS 858 is 0.5% of the load range: For the 222.41 N (50 lbf) load cell, this amounts to 1.11 N (.25 lbf). The tissue sample was mounted with the help of two aluminum blocks clamped together with four machine bolts on either side as shown in Figure 12. In order to hold the tissue in place the inner sides of the aluminum blocks were lined with a self-adhesive coarse grit tape (3M safety walk).

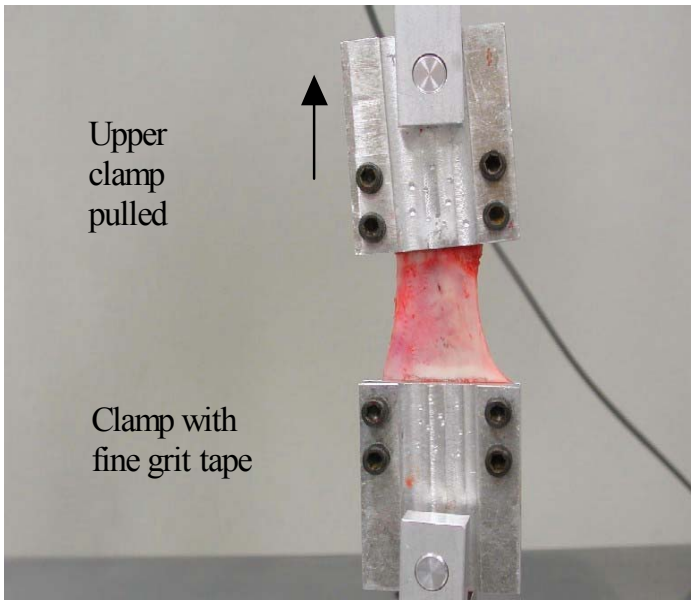

Figure 12 Sample mounted and clamped in the aluminum blocks with four machine bolts on either side.

Care was taken to maintain a consistent directional orientation for tissue samples: parallel to the long axis of the vaginal tissue for longitudinal measurements. Universal joints were utilized to grip the jigs with the tissue and ensure one directional loading. The samples were preloaded in tension to 2.224 N (0.5 lbs), to eliminate slack, and also to check for tissue slippage thus avoiding initial reading errors. Indelible ink marks were made on the tissue and tissue extension measurements were taken from this baseline to avoid edge-clamping errors. Sample length, thickness and width were recorded using a high precision digital caliper (Model #CD-6 CS, Mitutoyo Corporation, Japan) with ±0.01 mm precision. The tissue sample was loaded, under stroke control at a rate of 0.5 mm/sec. The tensile load was applied to the tissue via a force transducer (Eaton Corp, Model 3169-102) with a range of 222.4N (50 lbs). The accuracy of the load cell is 0.5% of the load range or 1.11N (0.25 lbs). Load-displacement data was collected at 4 Hz until specimen failure. The load and displacement data were digitally recorded (WinTest 2.5, EnduraTEC Systems Corp.).

All samples were carefully monitored during the loading process. In the event of slippage of the sample in the clamps, the loading was stopped and sample was re-clamped. The tissue dimensions were re-measured and then tested. The tensile loading of the tissue sample was sustained until tissue failure as shown in Figure 13.

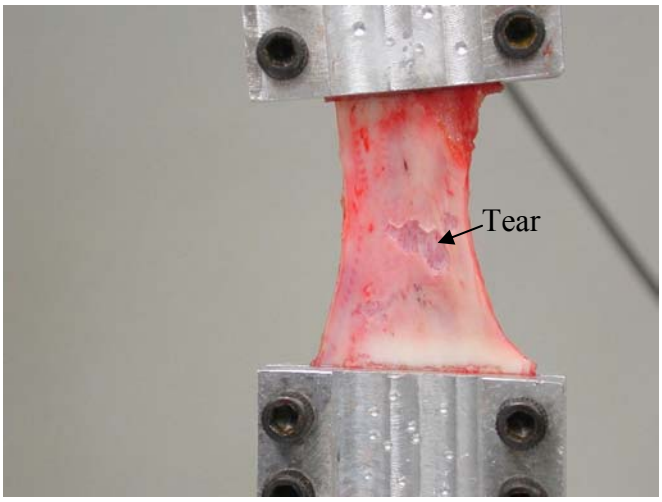

Figure 13 Clamped tissue showing a tear following loading to failure

The tear site on the tissue was clamped in muscle biopsy forceps for preserving the tear site. The clamping jigs were unloaded with the preserved tear site in the muscle biopsy forceps. The tissue specimen was then released from the aluminum clamps and immersed in Streck Tissue Fixative (STF), (Streck Laboratories Inc., Omaha, NE) for subsequent histological and microscopic analysis. STF is a safe, effective fixative for histopathology. It provides distinct tissue morphology and tissue structure.

2.2.2 Mechanical analysis

The load and displacement data was obtained from the digital recorder (WinTest 2.5, EnduraTEC Systems Corp.). The physical dimensions of the tissue were measured before subjecting the tissue to uniaxial load. The cross sectional area of the tissue is obtained from those dimensions. From the raw data the stress and strain was calculated by using the following formulae:

Stress = load / cross sectional area of sample

Example: load = 30 N

Area= (length of tissue being tested) *(thickness) = 11*2 = 22

Stress = 30/22 = 1.36 N/mm^2

Strain= Change in length (Δl)/ original length (l)

Example: Change in length, Δl = 2mm

Original length, l = 4mm

Strain= 2mm/4mm=0.5

The stress and strain curves were then plotted. Figure 14 shows a typical stress-strain curve obtained when the tissue was subjected to uniaxial tensile loading.

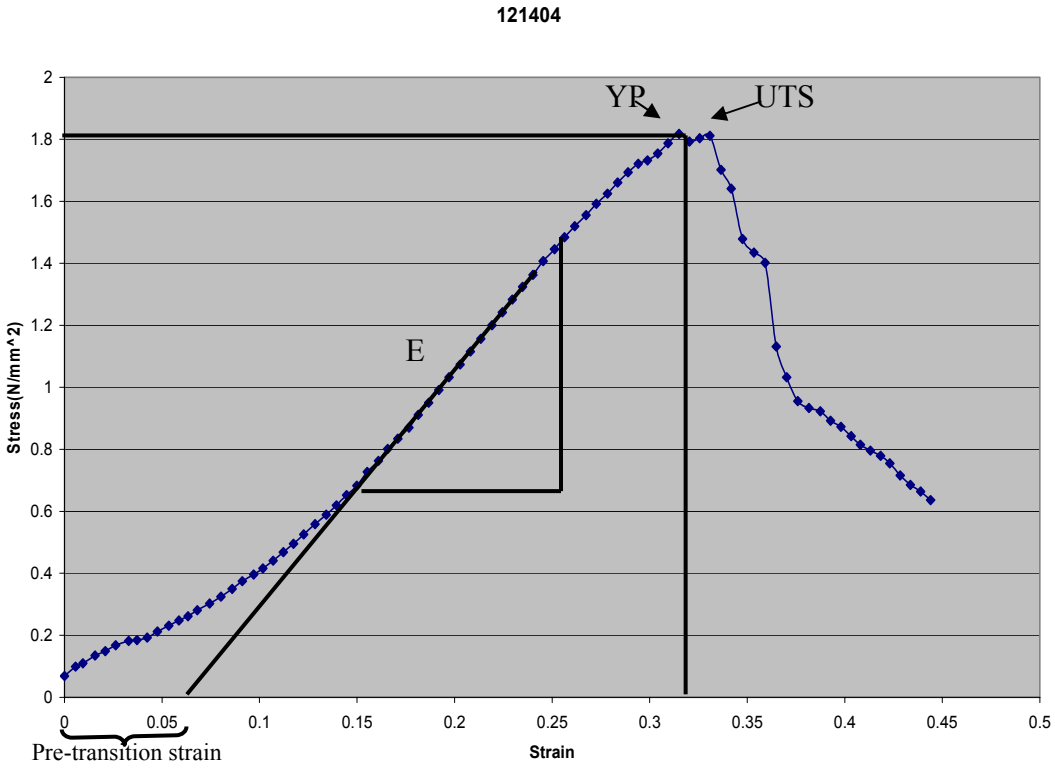

Figure 14 Typical stress strain curve obtained for tissue subjected to uniaxial loading

The Young's modulus was calculated from this curve. It can be calculated mathematically as:

Young's Modulus=Stress/Strain

As shown in Figure 14 the slope of the linear region of the stress-strain curve provides the Young's Modulus (E). The yield point and the ultimate tensile stress were easily obtained from the stress-strain curve. The pre-transition regions of the samples were also measured where the linear portion of the stress-strain curve was extended towards the x-axis and the x-intercept was measured (Figure 14). The equation of the straight portion of the curve was obtained to be of the form y=mx+c. A value of y as zero was assigned and the x-intercept was calculated.

The effect of hydration in the tissue samples was analyzed. The young's modulus, ultimate tensile stress and the yield point of the tissue samples were calculated and compared. The twenty-three prolapse samples that were transported in gauze moistened with saline were compared to the three control samples.

2.3 Light and Electron Microscopy Analysis

The main aim of this analysis was to:

1) Compare the tissue characteristics of the prolapsed anterior vaginal wall tissue with those of control tissue.
2) Study the ultrastructure of prolapsed anterior vaginal wall tissue, i.e. orientation of the collagen bundles, diameter and periodicity of collagen fibers in prolapsed tissue samples.

2.3.1 Specimen Preparation

2.3.1.1 Light microscopy

Samples of non-stretched and stretched anterior vaginal wall measuring 1.0x1.0x0.5cm were immersed and fixed in STF (Streck Laboratories Inc., Omaha, NE) for 24 hour. Tissues were processed according to a routine automatic tissue processing cycle (See Appendix B) on a Shandon Hypercenter XP automated tissue processor (Thermo Electron Corporation, Waltham, MA). Tissue blocks were oriented and embedded in paraffin wax moulds on a Shandon embedding center. The paraffin blocks were sectioned at 4μm on a Finesse microtome (Thermo Electron Corporation, Waltham, MA). Sections were mounted on clean glass microscope slides and dried in oven overnight at 60°C. Paraffin sections were stained using the haematoxylin and eosin (H&E) stain, (see Appendix C) [9]. Sections were examined on an Olympus BX40 light microscope; representative digital images were taken with an Olympus DP70 digital camera. Epithelial layer thickness was measured from the digital images with AxisVision software and recorded as an excel file.

2.3.1.2 Electron Microscopy

Strips of non-stretched anterior vaginal wall measuring 0.1x0.2x0.1cm were dissected under a stereo microscope and immersion fixed in 2% glutaraldehyde in 0.1 M cacodylate buffer with pH 7.4 at 4°C for 2 hours.

The sample of stretched anterior vaginal wall, after mechanical testing were clamped with muscle biopsy forceps to maintain stretched conditions. They were immersed in STF and transported to the Pathology lab. Section of tissue damaged by

the clamp were dissected off and discarded. Blocks of tissue measuring 0.1x0.2x0.1cm were dissected from the remaining tissues and fixed in 2% glutaraldehyde in 0.1M cacodylate buffer with pH 7.4 at 4°C for 2 hours. Both stretched and non-stretched samples were processed according to a routine EM automatic tissue processing cycle on a Leica automatic tissue processor (see Appendix D). Tissues were removed, oriented, embedded in fresh resin and polymerized in an oven overnight at 65°C.

The resin blocks were removed from the oven. Random blocks were sectioned at 1 μm using glass knife mounted on an ultramicrotome (Boeckler Instruments Inc., Tucson, AZ). Sections were dried on microscope slides and stained with 1% toluidine blue (TB) in 1% borax. The TB stain allowed assessment of the general structure and in the selection of areas for ultrasectioning [10]. The sections were studied for structural orientation by locating the epithelial layer and muscle layer. The area between the epithelium and muscle was the region of interest for this study.

Multiple 60nm thick ultrasections (silver) were cut on diamond knife (Drukker, Williston, VT). Ultrasections were collected on 200 mesh Athene copper grids (Electron Microscpy sciences), stained with Reynolds lead citrate and uranyl acetate and examined on a Zeiss 906 E electron microscope. Representative digital images were taken using a Keenview digital camera and ITEM computer software (Soft Imaging Systems, Denver, CO). Histomorphometric analysis was performed using the measurement macro.

2.4 Ultrastructural analyses

The diameter and periodicity was measured for the normal (stretched and non-stretched) and prolapsed (stretched and non-stretched) tissues. The area for the analysis was chosen as shown in Figure 15. The EM histomorphometry was performed using the macro of the ITEM computer software (Soft Imaging Systems, Denver, CO).

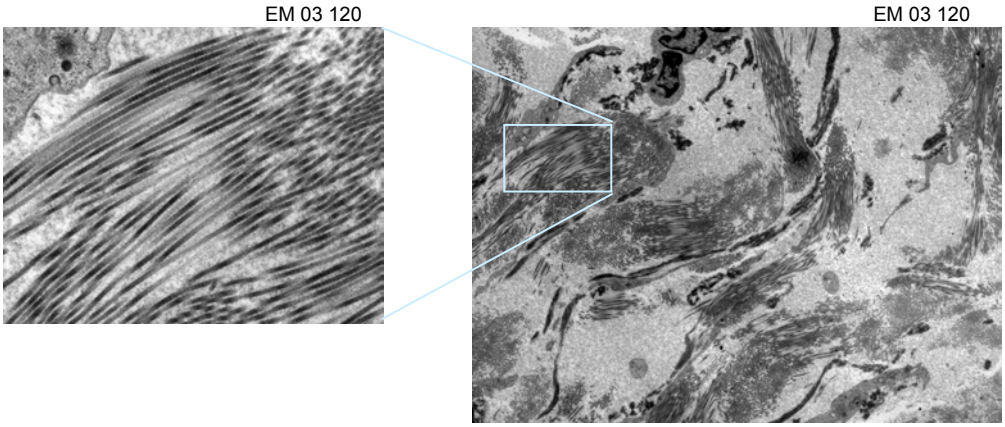

Figure 15 Selection of the area for measurements

The diameters of the normal tissue samples (both stretched and non-stretched cases) were measured and compared with those of the corresponding prolapse samples. Similar analysis was also performed for the periodicity of the fibers.

The Figures 16 and 17 show sample measurements of diameter and periodicity measured using the ITEM computer software (Soft Imaging Systems, Denver, CO) macro.

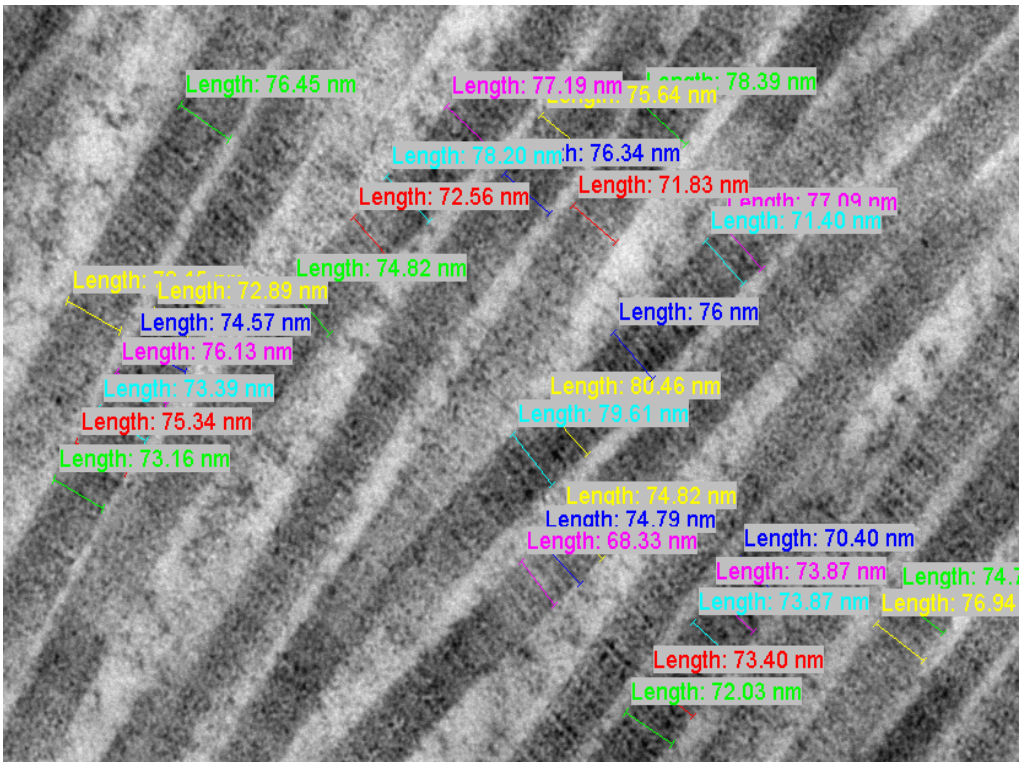

Figure 16 Diameter measurements for an unstretched control sample

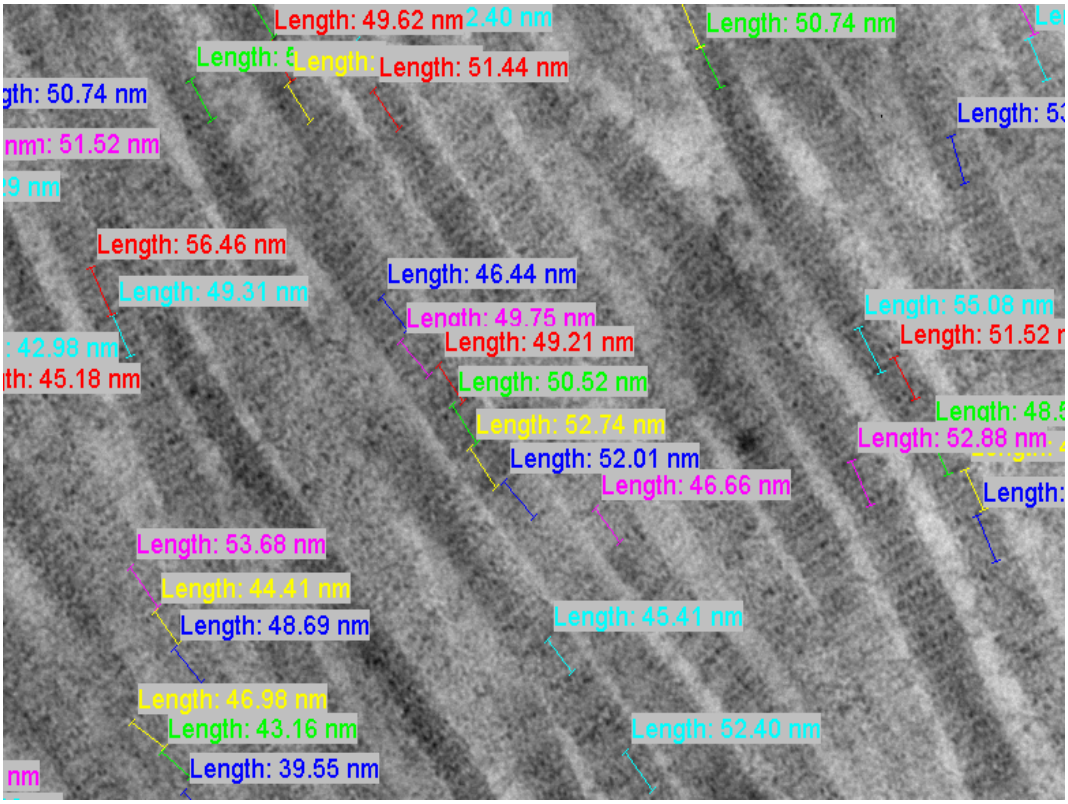

Figure 17 Periodicity measurements for an unstretched control tissue sample

2.5 Data analysis and statistical methods

For the mechanical analysis the Young's modulus, yield point and the ultimate tensile stress were recorded for all the samples. Yield point vs ultimate tensile stress, and young's modulus vs yield point were plotted for all the samples. The effect of hydration on the tissue sample was also analyzed as noted previously. The young's modulus vs yield point for the two groups was plotted. The first group comprised of tissue samples that were transported immersed in saline and the second group of tissue samples comprised the samples transported in gauze moistened with saline. Also the mechanical properties of the twenty-three samples transported in gauze moistened with

saline were compared to the three control samples that were obtained from asymptomatic females. The statistical method used to perform analysis was the standard student's t-test.

CHAPTER 3

RESULTS

A total of 42 samples were subjected to mechanical testing, control samples (n=3) and prolapse samples (n=39). Young's modulus, ultimate tensile stress, yield point and the pre-transition strain were obtained from the stress- strain curves for all the samples. The influence of hydration on the tissue samples was also analyzed. The structure of control and prolapse samples were studied by light microscopy. Collagen fiber diameter, periodicity and orientation, along with the elastic fiber morphology were analyzed with the aid of transmission electron microscopy. Clinical data, excluding age that might relate to the tissue properties was withheld, according to the rules governing this IRB-approved study.

3.1 Mechanical analysis

3.1.1 Patient age

The age distribution for the prolapse patient sample was 52-85. The mean age for the entire population was 69.3 ± 9.8 (mean ± SD) years. The patient age distribution for the two groups identified as group 1 and group 2 are shown in table 2. The grouping is done based on the tissue hydration level as described in chapter 2. The mean age of the control patients is also shown in Table 2. One control sample was used for histological study (84 year old).

Table 2 Patient age distributions for group 1, 2 and control group

	Patient age (mean± SD)
Control Group, (n=3)	72.3±13.2
Group 1, (n=16)	68.9±9.5
Group 2, (n=23)	69.7±10.3

3.1.2 Tissue thickness

The average thickness of the anterior vaginal wall tissue biopsies of group 1 (n=16) samples, group 2 (n=23) samples and the control samples are shown in Table 3.

Table 3 Tissue thickness for group 1, 2 and control group

	Tissue thickness (mm) (mean±SD)
Control (n=3)	2.7±0.4 ^{NS}
Group 1(n=16)	3.2±1.2
Group 2(n=23)	2.2±0.8 ^{NS}

A standard Student's t-test was performed and it indicated that the difference in the tissue thickness between group 1 and group 2 was not statistically significant. Similar result was obtained when the control samples were compared to group 2. Group 1 samples were not compared to the control samples due to the difference in the mode of tissue transport.

3.1.3 Pre-transition strain

The pre-transition strain was measured for all the samples as described in chapter 2. The pre-transition regions for group 1, group 2 and the control group are summarized in Table 4. A Student's t test for unequal variances was conducted in order to determine the statistical significance in the readings. Group 1 samples were not compared with the control samples due to the difference in the mode of tissue transport.

Table 4 Pre-transition strain for group 1, 2 and control group

	Pre-transition strain (mean±std dev)
Control (n=3)	0.003 ± 0.02^{NS}
Group 1(n=16)	0.019 ± 0.05
Group 2(n=23)	0.03 ± 0.06^{NS}

3.1.4 Young's modulus

The Young's modulus was calculated for group 1, group 2 and control samples. A standard Student's t-test was conducted to determine the statistical significance of Young's modulus for the group 1 and group 2 samples. Similarly the Young's modulus for group 2 sample and control sample was compared. Control samples were not compared to the group 1 samples due to the difference in the mode of tissue transport. Table 5 shows the values of the moduli for group 1, group 2 and the control samples.

Table 5 Young's moduli for group1, 2 and control group.

	Young's modulus (N/mm^2)
Control (n=3)	10.2±3.8 ^{NS}
Group 1(n=16)	4.4±2.8
Group 2(n=23)	8.4±4.8*

* $p < 0.001$

To investigate the influence of hydration on Young's modulus they were plotted for all the samples in group 1 and group 2. The results obtained are shown in Figure 18.

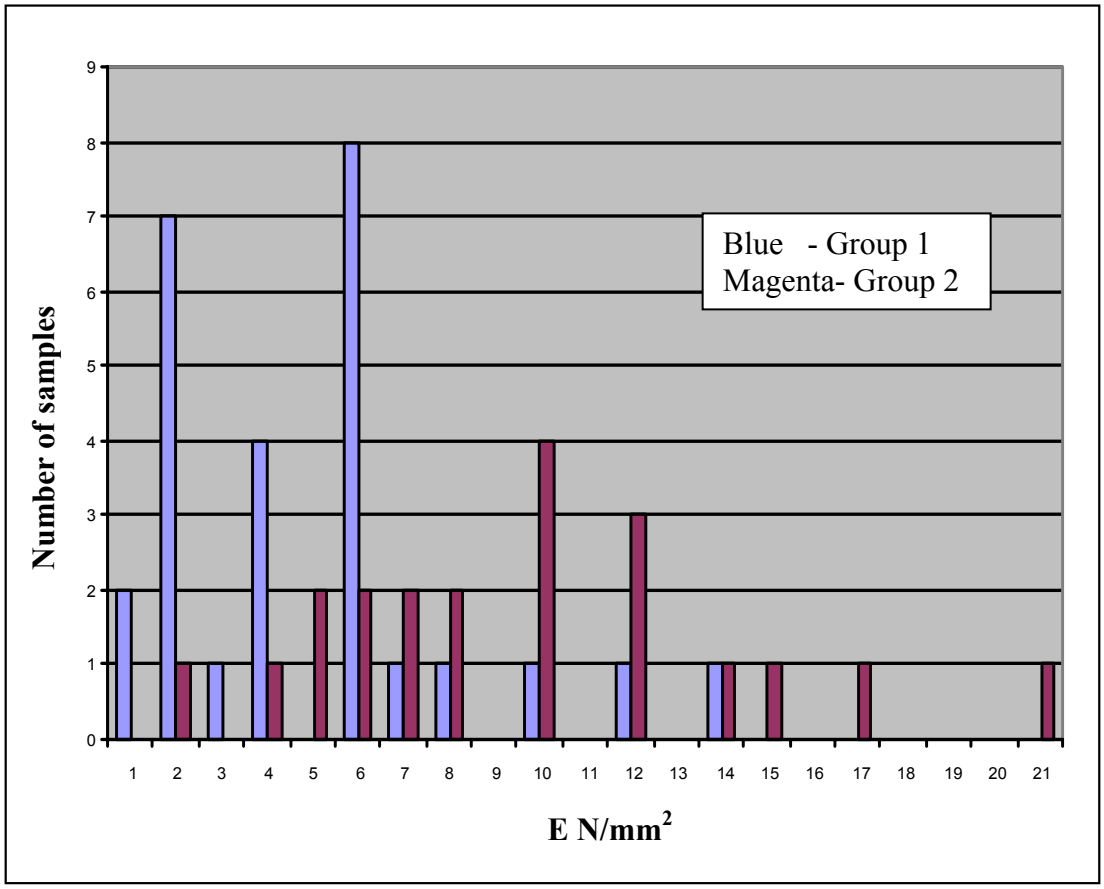

Figure 18 Histogram indicating the influence of hydration on Young's modulus of prolapsed anterior vaginal wall

3.1.5 Yield point

The yield points for the samples in group 1 and group 2 were calculated and a standard student's t-test was performed to determine the statistical significance of the results. Similar test was conducted on the group 2 and control samples. The yield points for group 1, group 2 and control samples are shown in Table 6.

Table 6 Yield point values for group1, group 2 and control group.

	Yield point (mean±SD)
Control (n=3)	0.13±0.05**
Group 1 (n=16)	0.5±0.2
Group 2(n=23)	0.3±0.2*

*p<0.02, **p<0.003

The yield point and the young's modulus for the samples moistened with gauze are cross-plotted and the results are shown in Figure 19.

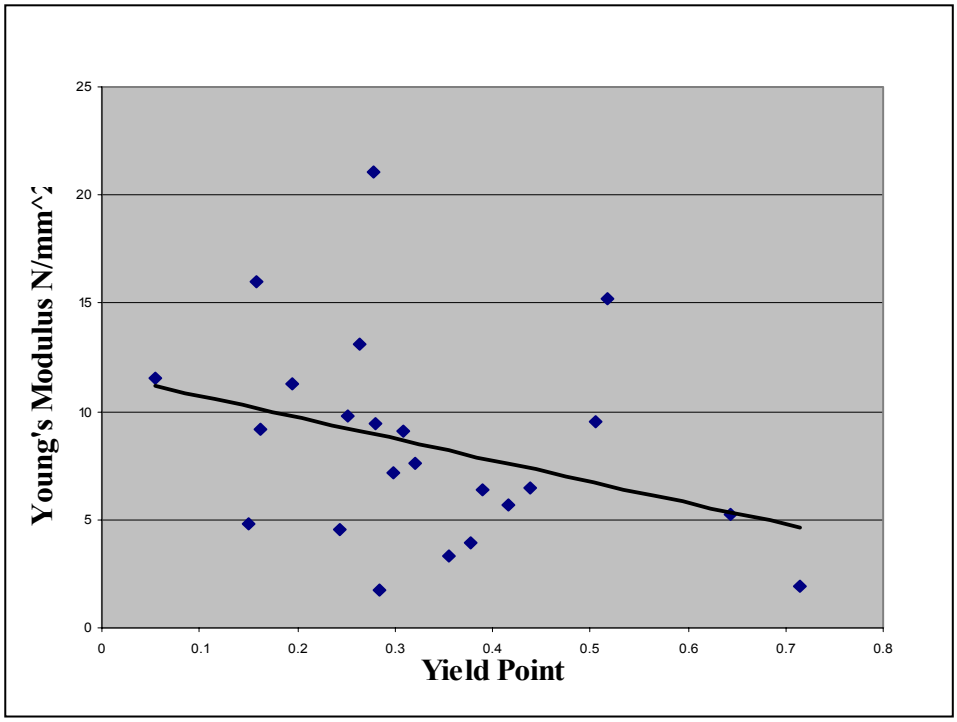

Figure 19 Scatter plot of the yield point and the Young's modulus plotted for group 2

The yield point and the Young's modulus for the samples moistened by immersion in saline are cross-plotted. The results obtained are as shown in Figure 20.

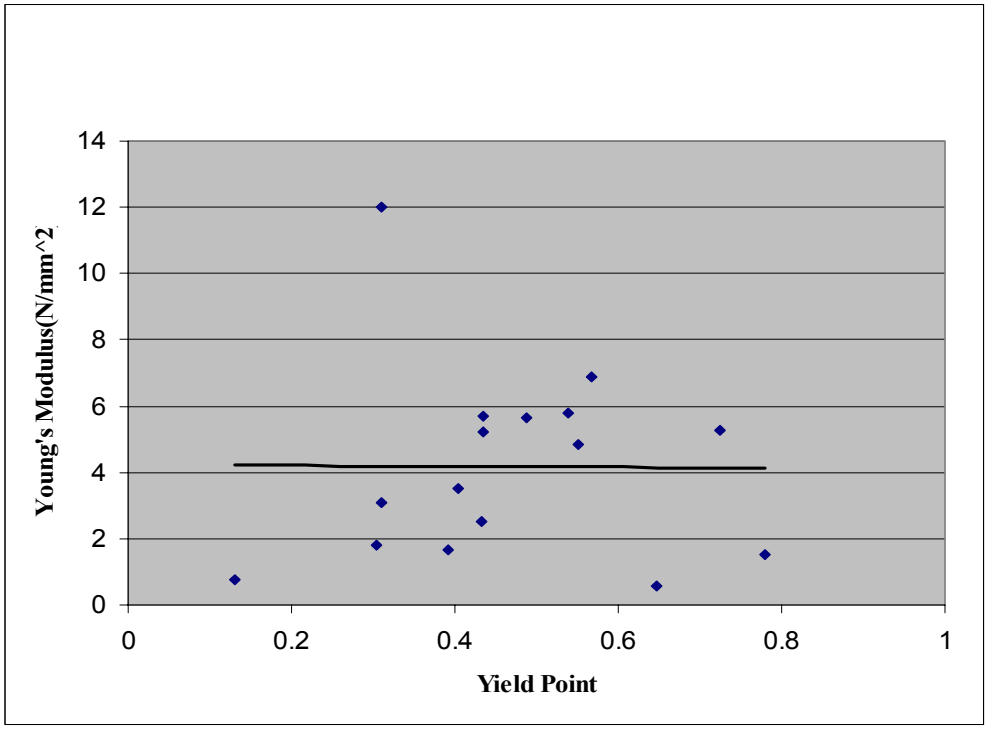

Figure 20 Scatter plot of the yield point and the Young's modulus plotted for group 1.

3.1.6 Ultimate tensile stress

The ultimate tensile stress was calculated for all the samples in group 1, group 2 and the control samples. The data obtained was tabulated and analyzed using the standard student's t-test. The results are shown in Table 7.

Table 7 Ultimate tensile stress for group1, group 2 and control group

	Ultimate tensile stress (N/mm^2) (mean±SD)
Control (n=3)	1.4±0.4 ^{NS}
Group 1 (n=16)	1.4±0.2
Group 2 (n=23)	2.1±0.3 *

*p<0.03

The ultimate tensile stress for all samples are plotted against the yield point and shown in Figure 21, which indicates a positive correlation.

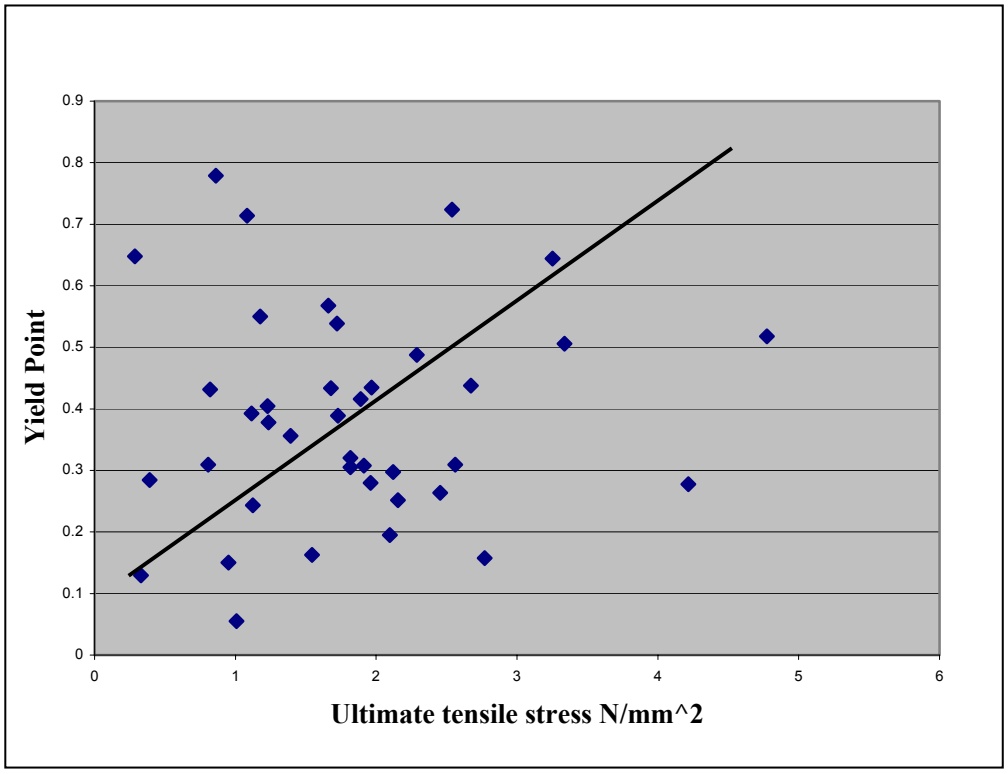

Figure 21 Ultimate tensile stresses for all samples, irrespective of their hydration level

3.2 Light microscopy analysis

Multiple 4 µm thick H&E stained sections were obtained from the paraffin blocks prepared from control and prolapsed tissues. Stretched and unstretched stained microscope sections were examined from prolapse and control tissue sample. The digital images of the unstretched (Figure 22) and stretched prolapse (Figure 23) samples of the anterior vaginal wall were taken. The smooth muscle bundles are seen oriented in tangential and longitudinal section. The adventitia, consisting of dense connective tissue with many elastic fibers is seen along the excision margin showing charring artifact due to dithermia (Figure 22).

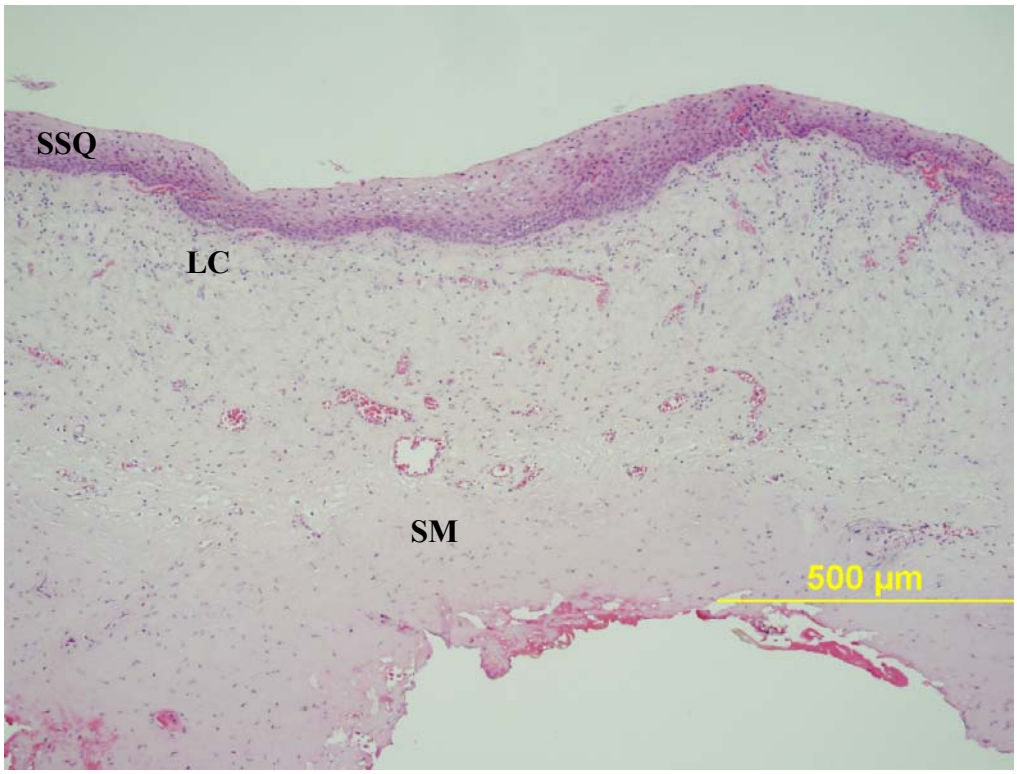

Figure 22 Digital image of the cross-section of unstretched prolapse sample (mag. x 10), showing a thick epithelium. SSQ-Stratified Squamous Epithelium, LC-Loose Connective tissue layer, SM-Smooth Muscle layer.

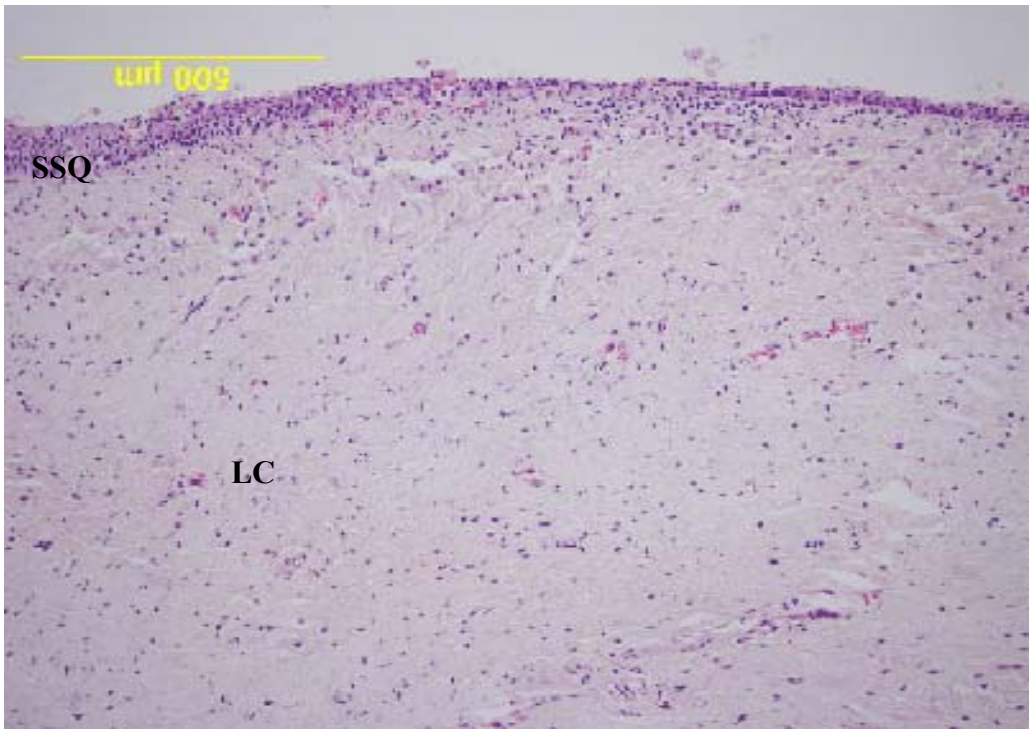

Figure 23 Digital image of the cross-section of stretched prolapse sample (mag. x 10) showing a thinned out epithelium. SSQ-Stratified Squamous Epithelium, LC-Loose Connective tissue layer.

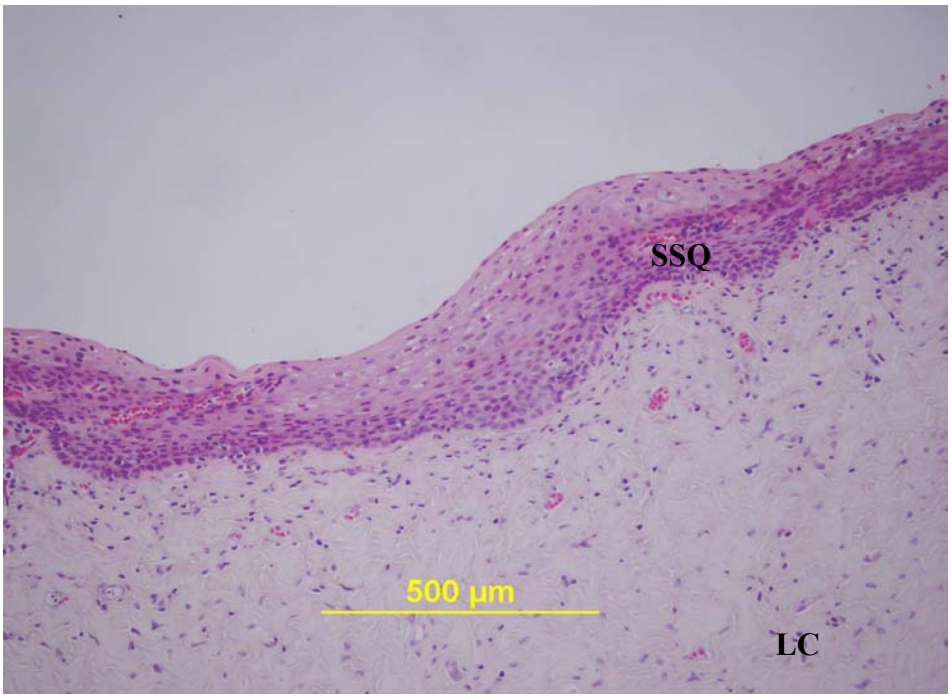

(a)

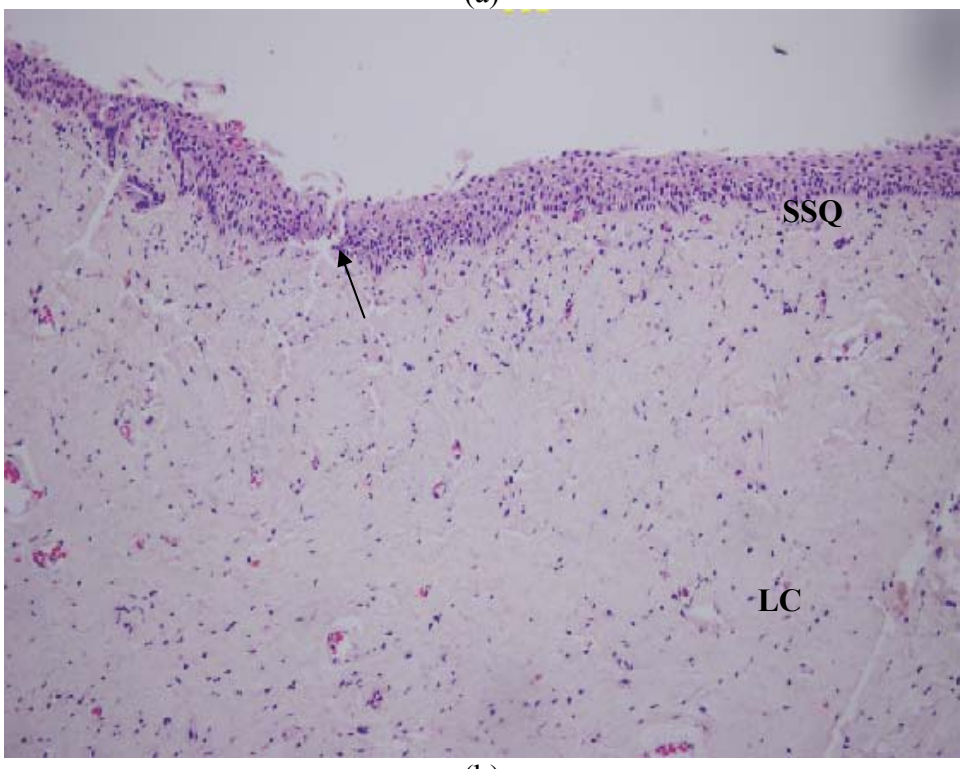

(b)

Figure 24 Digital images showing the relative thickness of the epthelium of the (a) unstretched and (b) stretched prolapse sample (mag. x 20). Arrow (→) indicates epithelial tear. SSQ-Stratified Squamous Epithelium, LC-Loose Connective tissue layer.

On examination the mucosal layer of the prolapse unstretched samples, they revealed a normal stratified epithelium, which was twice the epithelial thickness of the stretched prolapse sample. A standard student's t-test was conducted; the results obtained were statistically significant (Table 8). See Appendix G for the set of data generated.

Table 8 Thickness of the epithelium in unstretched and stretched prolapse sample

	Thickness of the epithelium (μm)(mean±SD)
Unstretched prolapse tissue	72±4.8
Stretched prolapse tissue	30.5±4.2*

*$p<0.00001$

A loose connective tissue with many elastic fibers is found underneath the vaginal epithelium. A rich vascular supply is seen. In comparison, the stretched samples showed substantial thinning of the stratified squamous epithelium, with small central tears and portions where the epithelial is missing. Papillae formation was seen on another unstretched prolapse sample shown in the Figure 25.

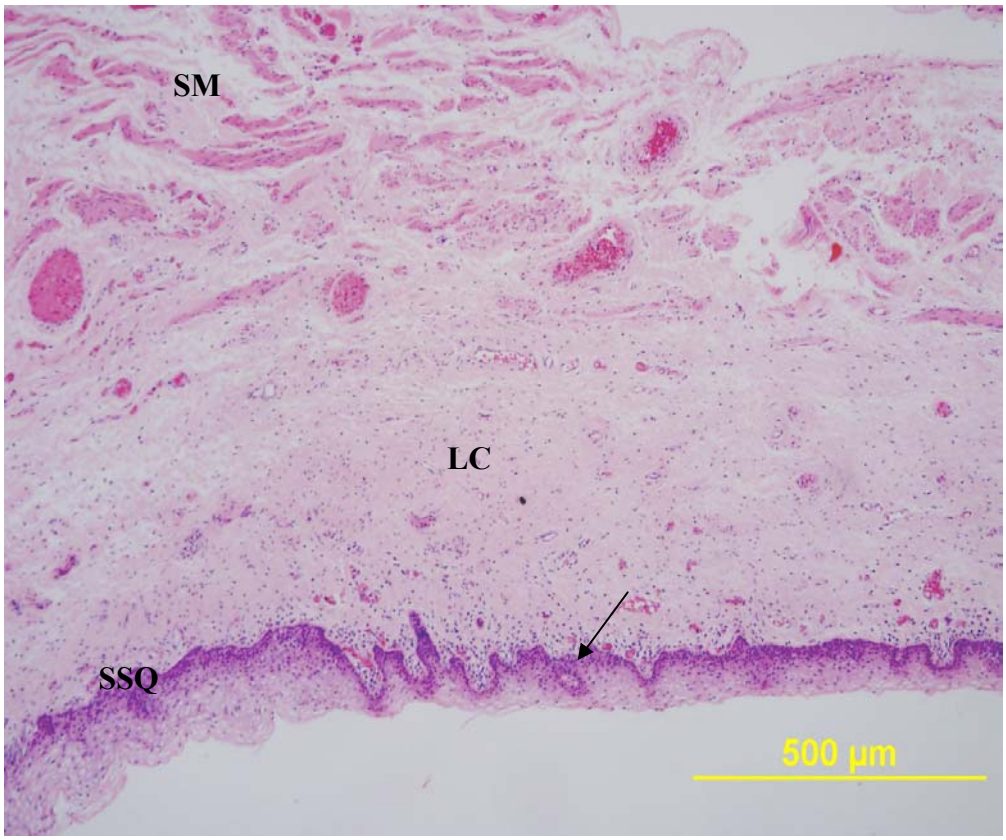

Figure 25 Digital image showing papillae formation as seen in the unstretched prolapse sample from an 84-year-old patient (mag. x 10) Arrow (⟶) papillae. SSQ-Stratified Squamous Epithelium, LC-Loose Connective tissue layer,SM-Smooth Muscle layer

Two samples obtained from a female subject who showed symptoms of anterior vaginal wall prolapse. One piece was transported by immersion in saline (Figure 26(a)) and the other was wrapped in gauze slightly moistened in saline (Figure 26(b)). These samples were subjected to uniaxial load. They were sectioned and stained with H&E. The loose connective tissue layer showed evidence of stretching. The collagen shows splitting of the collagen aggregates and an increase in micro interstitial spaces (Figure 26 and 27).

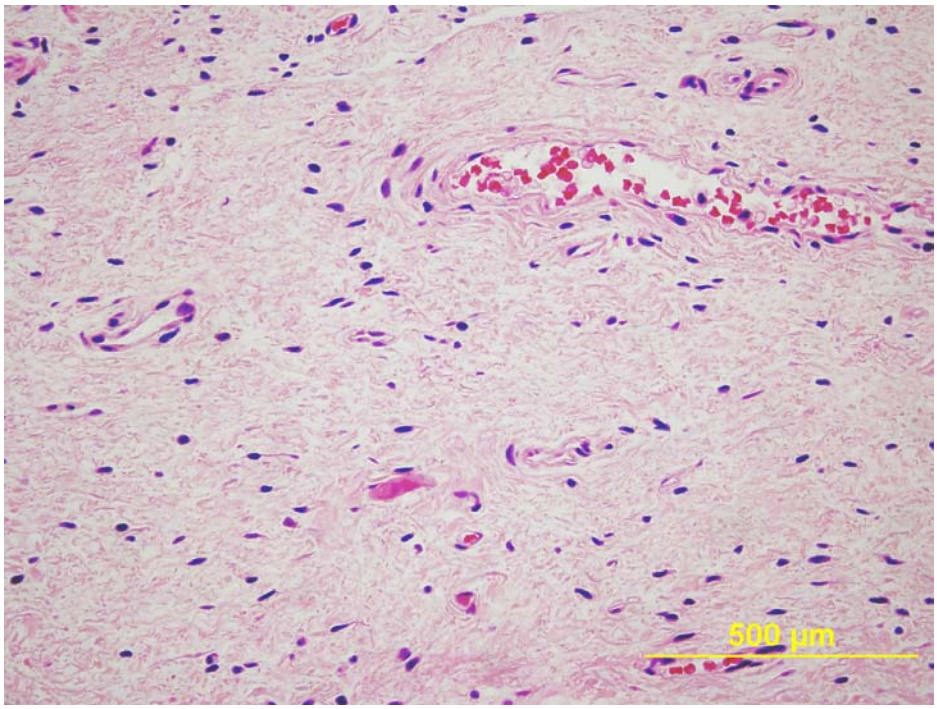

(a)

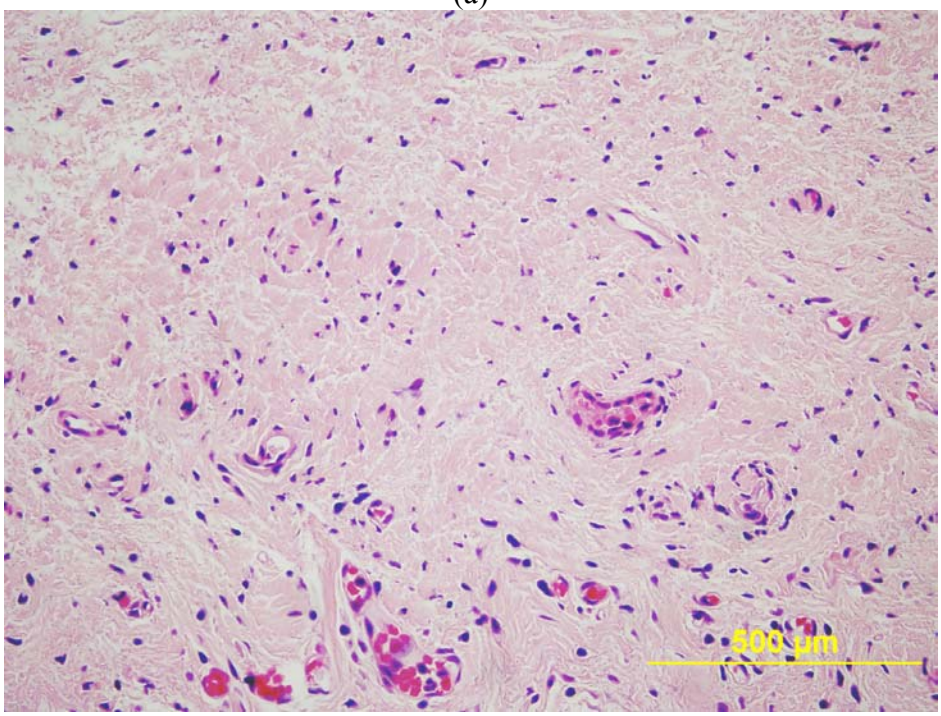

(b)

Figure 26 High power digital images of the cross section of (a) sample immersed in saline showing void spaces (mag. x 20) and (b) sample wrapped in saline moistened gauze (mag. x 20).

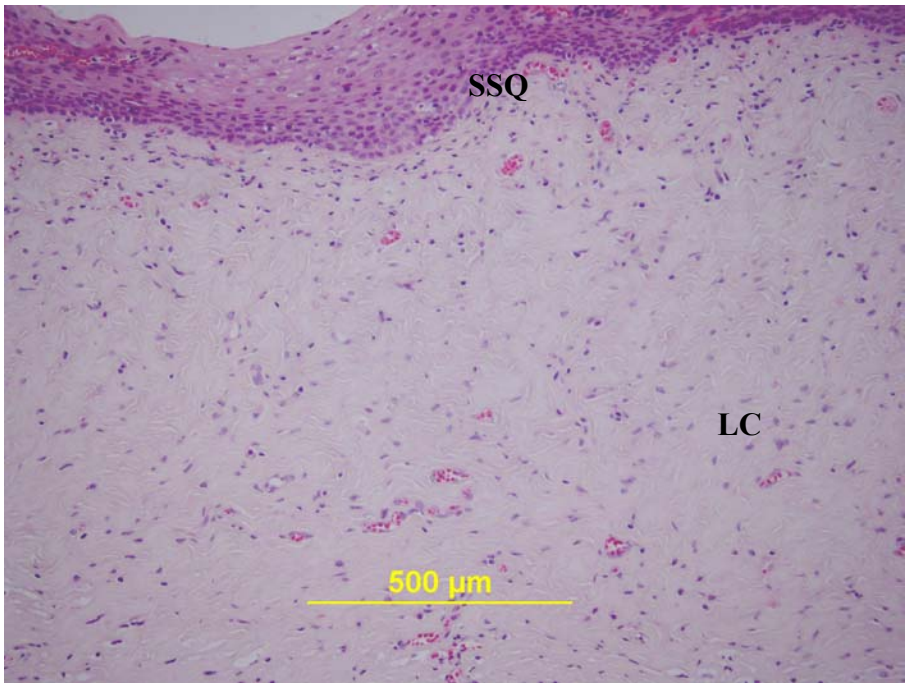

(a)

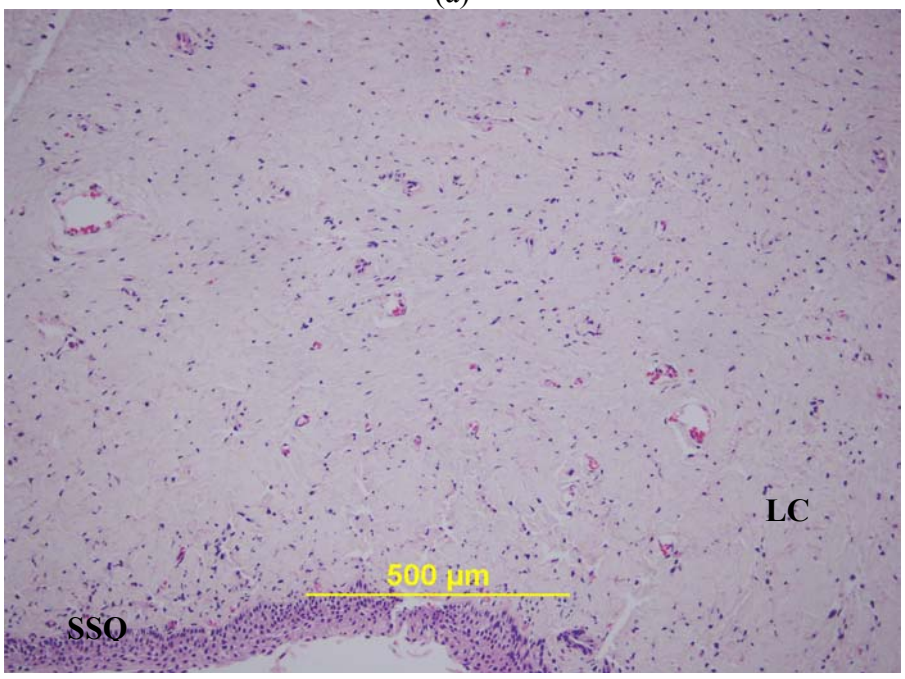

(b)

Figure 27 Low magnification digital images of areas that were chosen for EM analysis exhibiting (a) regions of organized loose connective tissue layer in the unstretched sample (mag. x 20) (b) various interstitial spaces due to stretching of the prolapse sample showing a tear in the epithelium (mag. x 20) SSQ-Stratified Squamous Epithelium, LC-Loose Connective tissue layer.

3.3 Ultrastructural analysis

3.3.1 Electron microscopy analysis of moistened samples of anterior vaginal wall

Ultrastructural analyses was performed on two gauze-stored tissue samples, one control sample and an age-matched, prolapse sample (Group 2). The prolapse and control samples were obtained form patients who were 85 and 84 years old, respectively.

Ultrathin sections from the resin embedded blocks of vaginal wall which was taken from the loose connective layer of the mucosal surface showed tightly packed aggregates of collagen bundles. There were long and unfragmented electron dense elastic fibers present in the unstretched sample (Figure 28a). In comparison, the ultra thin stained sections taken from the stretched tissue showed loosely packed and disorganized collagen bundles. Several areas were devoid of ultrastructure. The elastic fibers were semi electron dense showing varying degrees of fragmentation (Figure 28b).

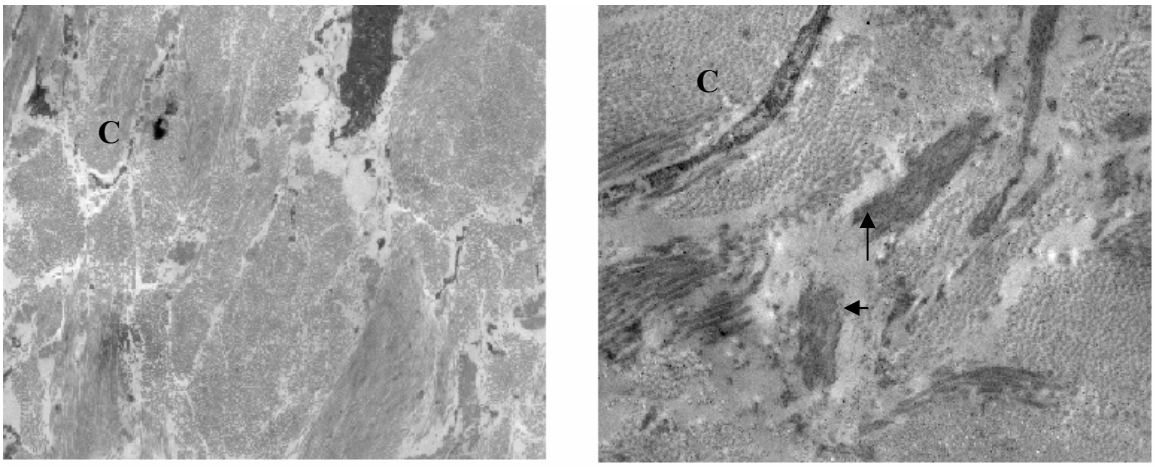

(a) (b)

Figure 28 (a) An electron micrograph taken from the loose connective tissue layer of (a) unstretched mucosal surface and (mag. x 1293) (b) stretched mucosal surface (mag. x 2784) of the anterior vaginal wall. Arrow (⟶) Elastic fibers; (C) collagen.

The analysis was performed on samples from the control group and group 2. Ultrathin sections were obtained from the loose connective tissue layer of the stretched and unstretched samples from the vaginal mucosa. The electron micrographs from the control sample revealed a uniform regular collagen fiber periodicity (51nm). The collagen bundles appear to be tightly packed in the control sample compared to the stretched and unstretched samples. The collagen fibers formed a complex, irregular network but did not show evidence of breakage in all samples. In the control samples the elastic fibers appeared to be homogenous and electron dense (Figure 29(a), (c)). At high magnification the stretched and unstretched samples exhibited several areas devoid of ultrastructure.

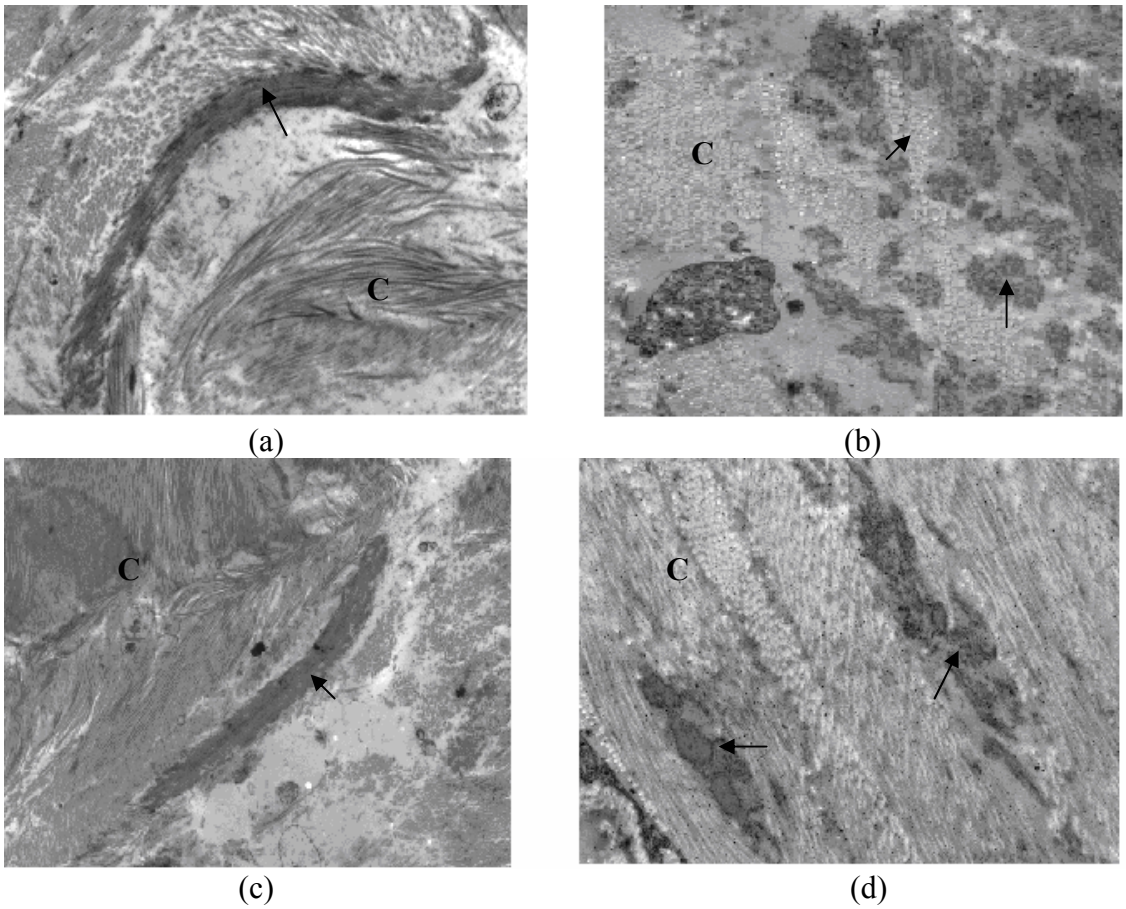

Figure 29 Electron micrographs showing the elastin morphology in (a) stretched control sample (x2156), the fiber is long and continuous and in (b) stretched prolapse sample (x2784), the fiber is fragmented.(c) stretched control sample (x 1293), the fiber is homogeneous and in (d) stretched prolapse sample (x2784), the fiber is non-homogeneous. Arrow (⟶) elastic fibers; C collagen.

There were 200 measurements generated for the collagen fiber diameter and 200 measurements generated for the periodicity using SIS software for the unstretched, stretched and control samples. The periodicity measurements for the stretched and unstretched prolapsed samples were 62nm and 60nm respectively. The control stretched and unstretched samples periodicity measured 54nm and 51nm respectively. The diameter of the collagen fiber, for the stretched and unstretched prolapse samples

were 63nm and 62nm respectively. The control samples that were stretched and unstretched, the diameter of the collagen fibers were measured to be 60nm and 70nm respectively. The average diameter and periodicity of the collagen fibers are shown in Table 9. A standard student's t-test was performed to determine the significance if the results were statistically significant.

All measurement data was saved as excel files, see appendix H.

Table 9 Average diameter and periodicity of collagen fibers for unstretched and stretched portions of the prolapse and control samples.

	Prolapse (mean ± SD)		Control (mean ± SD)	
	Stretched (nm)	Unstretched (nm)	Stretched (nm)	Unstretched (nm)
Diameter	$63.75\pm7.28^{*\&}$	$62.11\pm6.78^{**}$	$60.71\pm5.91^{+}$	70.23 ± 6.79
Periodicity	$62.61\pm6.57^{*\&}$	$60.37\pm4.43^{**}$	$54.71\pm3.08^{+}$	51.19 ± 3.95

* $p< 0.0001$ stretched prolapse vs. stretched control
** $p< 0.0001$ unstretched prolapse vs. unstretched control
& $p< 0.0001$ stretched prolapse vs. unstretched prolapsed
+ $p< 0.0001$ stretched control vs. unstretched control

CHAPTER 4

DISCUSSION

The main aim of the study was to obtain both biomechanical parameters and histomorphological characteristics of the anterior vaginal wall tissue in order to understand the pathophysiology of the disease. The biomechanical parameters, connective tissue morphology and histomorphometry measurements performed in this study are key factors in the understanding of the failure mechanisms of the anterior vaginal wall due to bladder prolapse. Analysis of the data indicated that there is an association between the mechanical properties of the tissue and it's morphology.

The function of the extracellular matrix is to serve as a scaffold for cells of the tissue, determine the biomechanical properties of tissues and provide a reservoir of growth factors and cytokines. Thus the extracellular matrix determines the tensile strength of the tissue and it's mechanical stability. Different types of collagens are predominant in this extracellular matrix, while the non-collagenous glycoproteins, elastin, hyaluronan and preoteoglycans are found in smaller amounts. Experiments by Boreham et al. indicated that the fibromuscular layer of the vaginal wall is altered in women with prolapse. Collagen type I and III are most abundant in the vaginal epithelium. Type I collagen form large fibers with high tensile strength. Type III collagen fibrils are smaller and more abundant in tissues that are highly distensible. The pelvic floor tissues undergo continuous tissue remodeling. The relationship

between the production and degradation of collagen is crucial to the tensile strength of the tissue [3]. Collagens are synthesized as soluble procollagen precursors, which are secreted and proteolytically processed to mature insoluble collagen molecules in the extracellular space. After synthesis on ribosomes, the α chains are subjected to numerous enzymatic modifications, including hydroxylation of proline and lysine residues. After the modifications, the procollagen chains align to form the triple helix. At this stage, the procollagen molecule is still soluble and contains N-terminal and C-terminal propeptides. During or shortly after secretion from the cell, procollagen peptidases clip the terminal propeptide chains, promoting formation of fibrils, often called tropocollagen, and oxidation of specific lysine and hydroxylysine residues occurs by the extracellular lysyl oxidase. This results in cross-linkages between α-chains of adjacent molecules stabilizing the array characteristic of the collagen [15].

The stress-strain relationships of soft tissues, like skin, artery and tendon, show a transition from a low modulus region at low strain to a high modulus region at high strain. These relationships have been related to the elastic properties of collagen and elastic fibers, commonly found in such tissues and in the anterior vaginal wall. Three regions can characterize the stress strain relationship of most soft tissues, as shown in Figure 30.

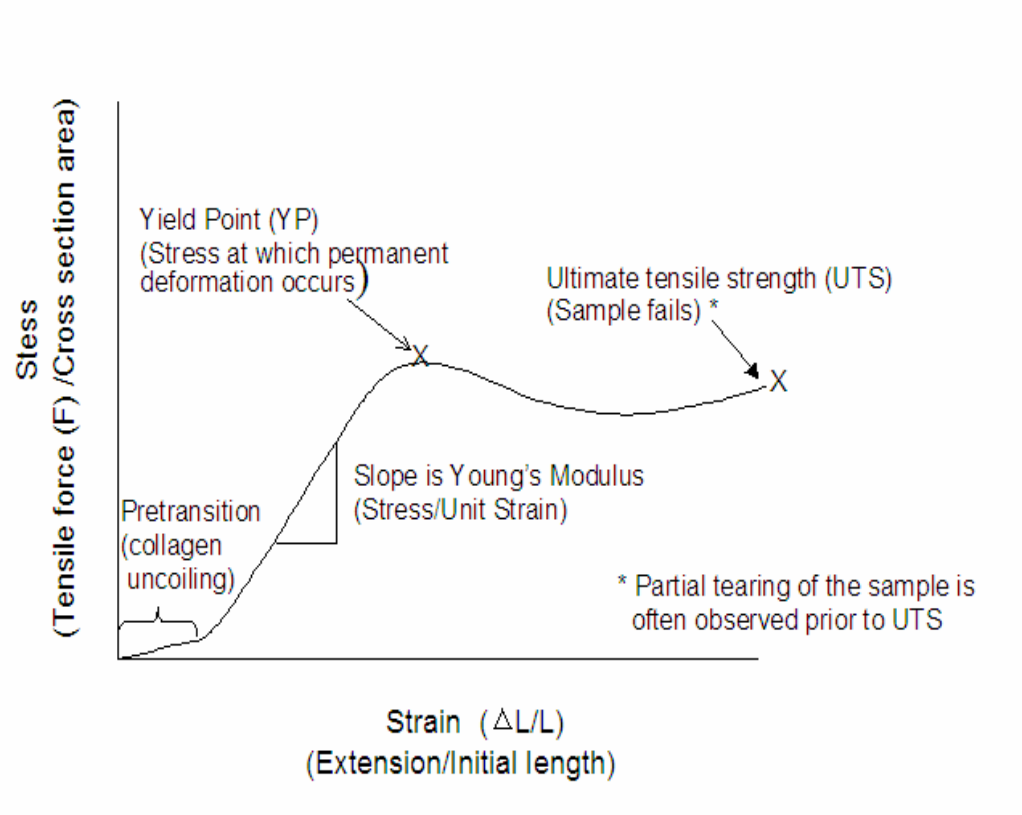

Figure 30 A typical Stress-strain curve

At low strain there is a region of relatively low elastic modulus in which large extensions may occur for small increases in applied load (pre-transition region). At high strain state there is a region of high elastic modulus in which extensions are much smaller for a given stress increment (post-transition). The elastic properties as given by Young's modulus (E, the local slope of the curve) in the pre- and post transition regions are approximately linear. In the middle region (transition) there is a change in the gradient of the stress- strain curve.

Since the elastic modulus of collagen is many orders higher than that of elastin, it is reasonable to assume that the load bearing properties of a tissue depend primarily on the arrangement of the collagen in the structure.

Tensile stress (σ) is calculated by normalizing the load to area, i.e:

$$\sigma = F/A_0$$

where: F= the applied tensile force

A_0 = the original cross-sectional area, normal to the applied force

Strain (ε) is calculated by normalizing the linear length increase to sample length, i.e:

$$\varepsilon = (L/L_0)$$

where: ΔL = change in length

L_0 = original length.

Collagen is a basic structural element in the soft tissues and hard tissues in animals. Therefore, the mechanical properties of the collagen are very important in the biomechanics of a tissue as demonstrated in the tissue under investigation in this study. The collagen matures to a high tensile strength matrix by the cross-linking of the collagen chains [11]. As viewed in an electron microscope the collagen fibers appear to be cross-striated with a definite periodicity. This was the basis of the EM analysis to compare the ultrastructural changes seen in the prolapsed group 1 and 2, and the control samples. There are different types of collagen present in the human body. The collagen type found in the samples of anterior vaginal wall under investigation in this study were types I and III [3].

The mechanical properties of the tissues in the prolapsed (stretched and unstretched) and control samples were found to be dependent on the organization of the collagen and elastic fibers, as well as cells and the ground substance within the anterior vaginal wall. This was supported by the results generated for the group 2 samples as compared to the group 1 samples. The group 1 samples that were immersed in saline absorbed fluid and impaired the structural strength of the tissue compared to the saline-moistened samples. This was shown in the data obtained from the biomechanical parameters. Thus proving that the female genital tract is more complex in its relationship between its structure and organization as stated by Fung et al [12].

The tissue samples that were harvested were not frozen. In the study conducted by Goh et al the vaginal tissue obtained from pre and postmenopausal females with prolapse were wrapped in saline soaked gauze and frozen. The tissue was thawed for an hour before being mechanically loaded [13]. Freezing the tissue wrapped in saline soaked gauze leads to the formation of freeze-induced needle-like crystals in and around the tissue. This leads to ice crystal artifact in tissue, which causes damage leading to improper measurements of mechanical parameters.

The thickness of the tissue under study was measured with a high precision digital caliper (Model #CD-6 CS, Mitutoyo Corporation, Japan) with ±0.01 mm precision. It was noted that the tissue thickness varied, depending on the mode of storage and transport (Table 3). In the tissue under investigation, anterior vaginal wall, Group 1 consisted of tissue samples that were immersed in saline during their transport. On macroscopic inspection and measurement it appeared to be thicker than the Group 2

samples that were wrapped in slightly moistened gauze. The immersion in saline seems to have caused swelling of the tissue due to absorption properties of collagen. The appearance of the Group 2 tissue samples resembled the freshly harvested tissue sample. On measurement they were thinner than group 1 samples. A tissue biomechanical analysis was conducted on two tissue samples to support the macroscopic finding.

Pre- transition strain is obtained from the stress-strain curve. It is the region on the stress-strain curve indicating the gradual straightening of the collagen fibers from their tightly intertwined state under the application of a load. The pre-transition strain values for group 2 and group 1 were not statistically significantly different (Table 4). However, the higher pre-transition region value for the samples wrapped in gauze moistened with saline (group 2) suggests that the collagen fibers absorbed less water and thus were able to better resist the applied load. Hyaluronic acid present in the connective tissue is known for its water-retaining property. The higher pre-transition strain for the group 2 tissue samples suggests that less saline was absorbed, therefore not over-hydrating the samples, consequently not weakening the structures due to saturation.

The Young's modulus (E) was significantly higher for group 2 ($p<0.001$, Table 5) suggesting that the prolapse tissue samples in group 2 were stronger compared to group 1. This was confirmed by the biomechanical study in which left vs. right segment preparation, differing only by saline immersion, showed a difference between the two samples, see Appendix F. The tissue samples in group 2 that were normally

distributed and the group 1 sample data skewed to the left (see the histogram of figure 18) supports these findings.

The yield point is the point beyond which the tissue undergoes irreversible damage. The yield point for the samples wrapped in gauze moistened with saline (group 2) was lower when compared to the samples immersed in saline (group 1). The results obtained were statistically significant ($p<0.02$) (Table 6). It is consistent with the scatter plot of YP Vs E from figure 19, which showed a decreasing trend for group 2 and with that of YP Vs E from figure 20, showed no change in the trend for group 1. It may account for the plastic deformation that is more easily accomplished for the better-organized fibers of group 2 than for the disoriented collagen fibers in the swollen environment of group 1.

The ultimate tensile stress (UTS) is significantly higher for group 2 tissues compared to those of group 1 (Table 7). UTS correlates with YP. As the yield point increases so does the UTS irrespective of the hydration level (from Figure 21).

The difference in percent elongation calculated for group 2 (50.6 ± 18.4) and control group (20.7 ± 4.1) shows statistical significance. The data indicates that the group 2 tissues elongated more that the tissue samples in the control group. The average stress-strain curves for these groups were plotted (Figure 31) and the elastic strain energy was calculated.

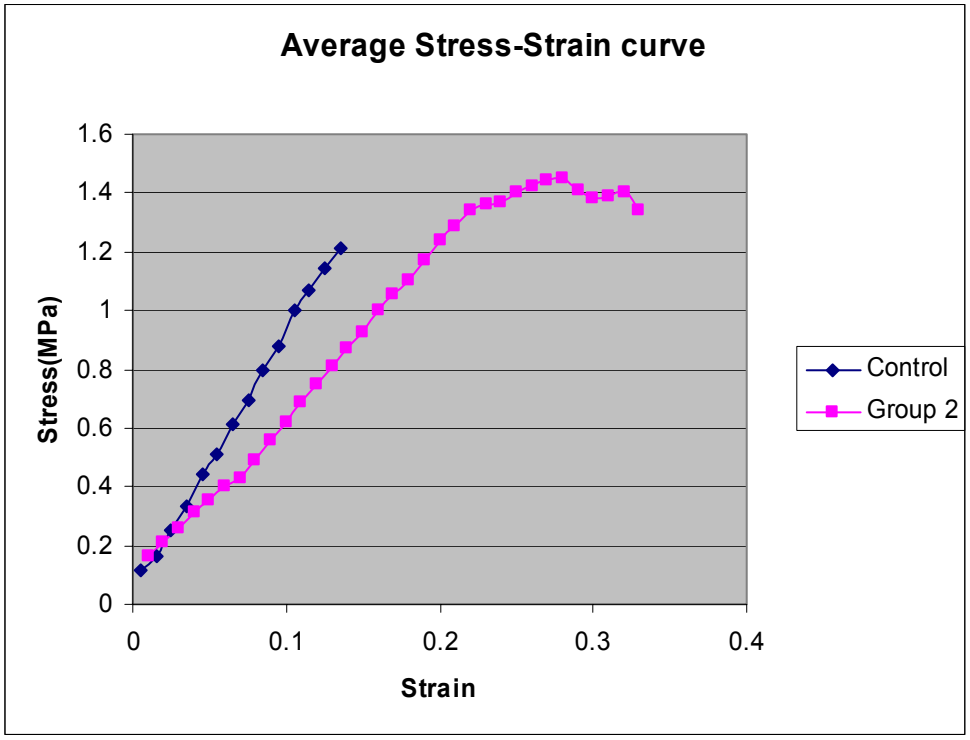

Figure 31 Average stress-strain curves plotted for control and group 2

The areas under the curves gives the elastic strain energy of the tissues comprising control group (0.09±0.003 J) and group 2 (0.31±0.004 J). The control group has lower elastic strain energy. A lower percent elongation with lower elastic strain energy indicates that the control tissues are stiffer than the group 2 tissues. However, more control samples are necessary for this observation to be firmed up to a conclusion.

The digital images taken of the H& E stained sections of unstretched prolapse samples revealed an intact epithelium, which was thicker with intact papillae formation (Figures 22, 24(a), 25). Those of the stretched prolapse samples showed the epithelium to be thinned out with absence of papillae formation (Figures 23, 24(b)). The images of the two samples that were subjected to two modes of transportation were obtained to

determine the effect of hydration on the tissue ultrastructure. The tissue sample that was stored by immersion in saline exhibited spaces in the interstitial matrix of varying sizes (Figure 25 (b)). The tissue sample stored in slightly moistened gauze did not exhibit the same degree of interstitial spaces within the matrix (Figure 25(a)). The stretched prolapse sample exhibited disorganization in the muscularis (Figure 27(a), 27 (b)).

The ultrastructural study showed that the mean diameter of the collagen fibers in the stretched control sample was significantly lower than that for the unstretched control sample. The mean periodicity of the collagen fibers in the stretched control sample was significantly higher than that for the unstretched control sample. This suggests that on the application of uniaxial load the collagen fibers were unwound and stretched causing thinning of the fibers and an increase in the periodicity. The diameter of the collagen fibers in the stretched, prolapsed sample (63.75±7.28nm) was significantly higher than that for the unstretched prolapse sample (62.11±6.78nm). The differences in diameters, though significant, are very close in range. To make a firm conclusion, further measurements should be performed on multiple samples to eliminate the possibility of tissue sample error.

The periodicity of the collagen fibers in the stretched prolapse sample was significantly higher than the unstretched prolapse sample. This suggests that stretching of the collagen fibers during uniaxial loading increased the periodicity of the collagen fibers.

Figures 32 and 33 summarize the major findings of the histomorphometry measurements.

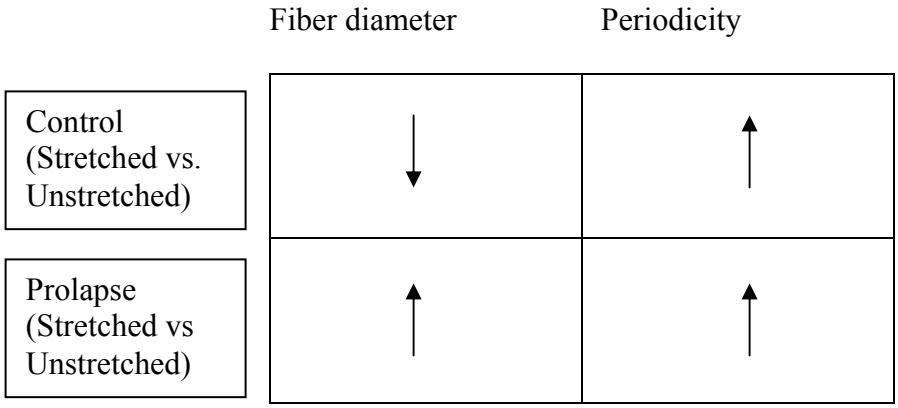

Figure 32 Latin square summarizes the findings for the control and prolapse samples

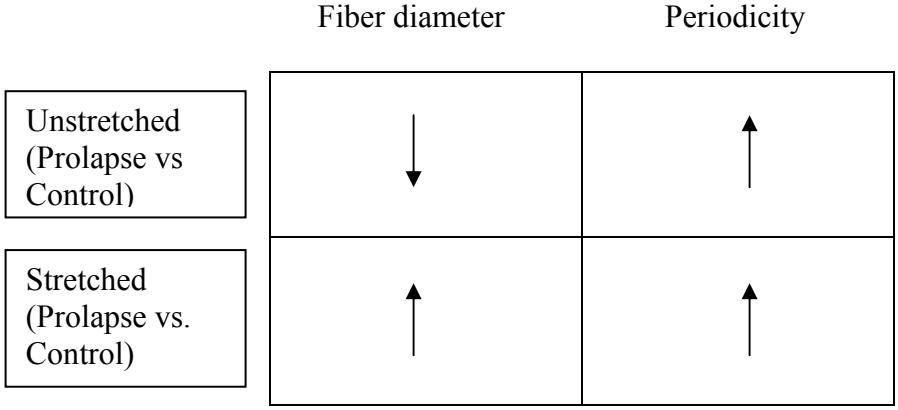

Figure 33 Latin square summarizes the findings for the unstretched and stretched samples.

The fiber diameter for the stretched prolapse sample should have been lower than that of the stretched control sample due to the effect of the application of the uniaxial load. This was not observed while making the measurements. This artifact could be an effect of tissue shrinkage due to dehydration during tissue processing [14] or due to the limitation of the clamping device mechanism of the Bionix 858 tester, which could allow for tissue slippage during stretching motion.

The elastic fiber morphology was abnormal in both the unstretched and stretched prolapse samples, which would indicate derangement of the elasticity of the anterior vaginal wall structure in prolapse. The elastic fibers appeared to be homogenous and electron-dense in the stretched control sample; in contrast, the elastic fibers appeared to be fragmented, with many void spaces in the stretched prolapse sample. Histomorphometric measurements of the elastic fiber length or thickness were not performed due to the limitations of the EM analysis. However, one can postulate that due to the abnormal ultrastructure of the elastic fiber, it would be a contributor to the tissue failure, i.e. loss of the elasticity.

In conclusion, the biomechanical testing, light microscopy, electron microscopy and histomorphometry measurements were supportive of the strong influence of the degree of hydration on the tissue samples. The prolapse tissue samples exhibited various spaces devoid of ultrastructure indicating that the stretching of the tissue samples under the uniaxial load caused tissue failure, preventing the collagen's natural elasticity in being able to recoil back to its normal state. The absorption of excess saline caused swelling of the loose connective tissue layer and possibly, the smooth muscle bundles, contributing to the weakening of the group 1 samples compared to the group 2 samples. The tissues of group 2 stretched slowly on application of load due to the gradual unwinding of the collagen fibers to bear the load and thus exhibiting higher pre-transition strain. At the same time in the group 1 samples, initially the collagen fibers were unable to bear the load until the absorbed fluid was removed by the application of the initial stretch, in essence, squeezing the samples "dry", leading to

lower pre-transition strain. When the uniaxial load was applied to the tissue samples, the group 1 samples underwent irreversible damage earlier than the group 2 samples. The ultimate tensile strength however was higher for the group 2 samples. The ultrastructural studies revealed a decrease in the diameter of the collagen fibers on the application of load. It suggests that the thinning of the fibers due to stretching caused the tissue to lose its elasticity and its ability to recoil back to its natural state. The diameter of the collagen fibers in the prolapse was lower compared to the control sample. This could be a factor in the failure of the tissue. Collagen alone is not responsible for tissue failure. Other extracellular matrix components, i.e. elastic fibers showed fragmentation by EM, which would be a contributing factor in tissue failure with loss of elasticity. The morphology of elastic fibers has been previously documented. This study conforms to the documented data [14].

With the steady increase in the aging population, life expectancy is longer and the pathological tissue failure of the anterior wall due to aging and trauma increases the national budgetary costs related to pelvic floor disorders. This will lead to higher health care costs, loss of productivity of patient and decreased quality of life. There is a lack of understanding of the pathophysiology of the pelvic floor disorders. In addition, there are a combination of risk factors, like childbirth and hormonal changes, which may lead to the culmination of these into a chronic clinical condition of a bladder prolapse. Knowledge of the true causes of this disorder will improve our understanding of the pathophysiology of the disease and prevention strategies can be arrived at. With the production of a biosynthetic support for prolapse repair thus preventing reoperation

which is estimated to be approximately 30% of the patients who underwent previous procedures [3].

CHAPTER 5

CONCLUSIONS

- Samples used in this study that were harvested and transported in gauze moistened with saline were more consistent with the appearance of freshly harvested tissue. This method of storage until the test was performed is concluded to cause less tissue damage from over hydrated saline immersion and less damage than freezing and thawing the tissue before mechanical testing.
- The tissue samples transported immersed in saline appeared to be weaker than the ones transported in gauze moistened in saline in terms of pre-transition strain and UTS. The over hydrated (saline immersion) samples yielded a statistically significantly lower Young's Modulus than those that were more properly prepared and transported on moistened gauze ($p<0.01$).
- The mechanical properties of the prolapse tissue samples appeared to be weaker than their normal counterparts in terms of pre-transition strain, Young's modulus, yield point and ultimate tensile strength. However sample size for the normal controls precluded statistical verification.
- The control sample exhibited normal ultrastructure. There was a regular periodicity and the collagen bundles seemed to be more closely packed than those of the prolapse samples. The elastin fibers appeared to be homogenous and electron dense.

- In contrast the tissue specimen for the prolapse case exhibited abnormal ultrastructure. There were a lot of void spaces; the collagen fibers seemed to form a complex, irregular network but were not fragmented. The elastin fibers appeared fragmented with a lot of void spaces.

CHAPTER 6

FUTURE STUDIES

The study conducted here is preliminary, and holds promise for revealing insights into the structure and function of prolapsed tissue to come. Certainly there are improvements to be made in many areas in order to obtain a clearer picture of the pathology of prolapsed tissue, and means to improve surgical correction.

The mechanical properties are important in the understanding the pathology of the disease. They could also be instrumental in building a working prototype for mesh that mimics the natural support structure.

The various components of the connective tissue matrix could also play a key role in the weakening of the tissue. The concentration of hyaluronan and other proteoglycans (lubricating agents) should be assessed in these tissues in order to determine if these factors remain involved in tissue movement and flexibility.

The ultrastructural studies were preliminary in nature. More work could be performed in the analysis of the tissue sample to obtain a good understanding of the ultrastructure of the tissue. Specifically, a three dimensional model should be prepared by analyzing the collagen and elastin densities and orientations in serial slices of the tissue sample and reassembling the array. The collagen and elastin densities should be calculated and compared for the non-prolapse control and prolapse samples. With the help of finite element analysis, the deformation under load of this 3-D re-assembled tissue with and without contributions from smooth muscle contraction could be

predicted. Such models could be instrumental in combining the mechanical parameters and the ultrastructural characteristics of involved tissues in the study of various pelvic floor disorders. Such model could also be adapted to urinary incontinence studies, because of their interdependence with vaginal prolapse disease.

The genetic aspect of the disease has not been considered in this study. This study, combined with an exploration of genes that transcribe the collagen or the elastin genes, especially, epigenetic analyses, might be helpful in the analysis of the pathophysiology of the disease.

The study could be narrowed down further to include the effect of hormonal therapy prescribed to the patients with various health conditions. The number of children borne by the patients could also be a factor.

APPENDIX A

IRB FORM

The University of Texas Southwestern Medical Center at Dallas
Institutional Review Board[1]

IRB Form NR1- EXP: Application for Review of Expedited Research
(Revised June 2001)

Title of Research[2]	Correlation between the biomechanical and histochemical properties of the human anterior vaginal wall
Sponsor and Grant Number[3]	The University of Texas Southwestern Medical Center, Department of Urology and Biomedical Engineering.

Assurances of the Principal Investigator and Sub-investigators

- To safeguard human subjects involved in this research, I agree to use procedures that conform to the policies of the University of Texas Southwestern Medical Center at Dallas and the regulations of the Department of Health and Human Services and the Food and Drug Administration.
- Unless it is necessary to eliminate apparent immediate hazard to a human subject, I shall seek prior approval from the Institutional Review Board (IRB) for substantive changes in the investigative procedures involving human subjects that may be called for during the research covered by this application.
- I shall agree to follow the advice of the IRB.
- I agree to report immediately to the IRB any unanticipated, life-threatening, or fatal complications with respect to human subjects.
- My signature certifies that I assure compliance with the ethical principles and institutional policies regarding the protection of human subjects in research as stated in Title 45 Code of Federal Regulations Part 46 (revised June 18, 1991; reprinted April 2, 1996) and the Multiple Project Assurance.[4]

Assurances of Department and Collaborating Chairmen

- I understand that responsibility for assessing the quality of research must be shared by both the department and the IRB.
- My signature certifies that I assure compliance with the ethical principles and institutional policies regarding the protection of human subjects in research as stated in Title 45 Code of Federal Regulations Part 46 (revised June 18, 1991; reprinted April 2, 1996) and the Multiple Project Assurance, and that I have reviewed the proposed research for the proper use of human subjects.
- This review encompassed experimental design, scientific merit, and accuracy of the proposed research.

Date of Application:

4/16/2002 P. Zinreich

[1]The IRB reviews all research involving human subjects for Children's Medical Center of Dallas, Parkland Health & Hospital System, Texas Scottish Rite Hospital for Children, the University of Texas Southwestern Medical Center at Dallas, St. Paul Medical Center, Moncrief Cancer Center in Fort Worth and Zale Lipshy University Hospital. The Board also reviews all research conducted at the Presbyterian Hospital of Dallas, The Retina Foundation of the Southwest and the Veteran's Affairs Medical Center of Dallas for which a member of the faculty at UT Southwestern serves as principal investigator.

[2]Title printed on the cover of the protocol, including the sponsor's protocol number, version, and date

[3]Complete name of the organization(s) funding the research

[4]Available as an electronic file at www2.swmed.edu/irb

Investigators' and Chairmen's Signatures

Name (printed)	Dept	Degree	Rank	Phone	Mail	E-mail	Signature
Philippe E. Zimmern Principal Investigator (PI)[5]	Urology	M.D.	Professor	89397	-9110	Philippe.Zimmern@utsouthwestern.edu	
Robert Eberhardt (Co Investigator	Biomedical Eng.	Ph.D.	Prof	82052	9130	Robert.eberhardt	
Victor Lin Co Investigator	Uro	Ph.D	Asst Prof	83924	9110	Victor.lin	
Claus Roerhborn Department Chairperson[6]	Urology	MD	Prof and Chair	82941	9110	Claus.roehrborn	

Please note that to qualify for expedited review, the research must present no more than minimal risk to human subjects and cannot explore sensitive topics. Designate below the category that qualifies this proposal for expedited review (click on http://www.swmed.irb/edu, "Local Guidelines", "Investigator's Manual" and then "Expedited Review" and "Approved Categories"), and justify this designation by responding to the statements below each category. The IRB will review your justification and decide if this study can be approved on an expedited basis. If it is decided that it doesn't meet expedited criteria completely, then you will be informed and submission of an NR1 form will be necessary.

Category #:

Information Required for Justification (specific information in attachments):

REC UTA GRAD SCHOOL APR 01 2005

1. Human vaginal wall excised as part of the vaginal wall surgery to correct the cystocele.

2. Material comes from each patient and will be collected prospectively.

1. PROBLEM UNDER INVESTIGATION:

Medical condition or scientific problem to be studied: Discover the unique properties of the human anterior vaginal wall with the hope of using this information to design an optimal mesh replacement.

Describe the research in simple language **by attaching a project summary** (template available on the IRB web-site). If this is a retrospective chart review (Category 5) (health records research) all of the following must be addressed: a) describe specifically what data (variables) will be extracted from each medical record, whether or not subject identifiers (name, medical record number, social security number, etc.) will be present, and at what point in time identifiers (if used) will be destroyed. Clarify how subject confidentiality will be protected. b) State why the research could not practicably be carried out without access to and use of the protected health information.

[5]Investigator responsible for the global aspects of the research. The IRB acknowledges one PI for a study.

[6]Chairman of the PI's or faculty sponsor's department (or center director)

2. SUBJECTS:

a) General Inclusion: All consecutive women undergoing surgery for cystocele repair in the next year.

Approximate number of subjects: 25 to 30

Age range (indicate whether months or years): 30 to 85

Gender: Male ( ) Female (X)

Explain below if either gender is excluded: Men do not have tissues analogous to the vaginal wall.

Will all racial/ethnic groups be included? Yes ( ) No (X) (If no, explain in project summary)
Please note that a consent document in the subject's own language will need to be provided.

Expected time to completion of enrollment or conclusion of study: One Year

b) Protocol inclusion criteria: None

c) Protocol exclusion criteria: None

Specify all classes of subjects included in the research:

Healthy volunteers: Medical students ( ), Center employees ( ), Minors (<18 yrs) ( ), Men ( ), Women (X)

Patients: Outpatients (X), Inpatients (X)

Vulnerable Subjects: Pregnant women ( ), Minors (<18 yrs) ( ), Men ( ), Women ( )
Cognitively impaired ( ), Terminally ill ( ), etc.

Other: Other class ( ) please explain below
Transvaginal repair of their symptomatic cystocele

3. RECRUITMENT:

Specify procedures for recruiting subjects: No particular efforts will be made for recruitment.

4. CONSENT OF SUBJECTS: Describe the method used to obtain informed consent. Prospective research ordinarily requires written informed consent. If any special subject classes are eligible to participate, discuss how the consent process will differ. Inclusion of children in minimal risk research requires permission of at least one parent and the assent of the child.

Tissue will be collected under the approved IRB file 0698-26900. Tissue will be surgical waste; no extra tissue will be removed for purposes of this study. The sample will not be identified, only numbered, demographic information and location of tissue will be recorded.

If requesting a <u>waiver</u> or <u>alteration of informed consent</u>, justify such in accordance with the following four criteria established under 45CFR46.116(d)(1-4):

1) The research involves no more than minimal risk* to the subjects? Yes ( ) No (X) **AND**

2) The waiver or alteration will not adversely affect the rights and welfare of the subjects? Yes ( ) No (X) **AND**

3) The research could not practicably be carried out without the waiver or alteration? Yes ( ) No (X) **AND**

4) Whenever appropriate, the subjects will be provided with additional pertinent information after participation? Yes ( ) No (X)

"*Minimal risk* means that the probability and magnitude of harm or discomfort anticipated in the research are not greater in and of themselves than those ordinarily encountered in daily life or during the performance of routine physical or psychological examinations or tests" (45 CFR 46).

Please note that the IRB will make the final determination if waiver of consent is appropriate.

5. RISKS AND BENEFITS:

Specify the risks and benefits to the subjects and/or society:

No risks to the subjects since that tissue would be discarded anyhow.
Benefits: refine our understanding of human vaginal wall properties with the hope of designing an optimal replacement mesh to repair bladder herniations.

6. CONFLICT OF INTEREST:

Is there a conflict of interest between any investigator and the sponsor?

Yes ( ) explain below and notify the Conflict of Interest Office
No (x)

7. PERFORMANCE SITES:

Specify the sites where (1) study procedures will be conducted, (2) patients will be seen, and (3) resources (equipment, supplies, personnel, etc.) will be utilized. Indicate whether Form NR2 has been sent to the appropriate authority at the performance site.

Performance Site	Recruitment	Resources	Form NR2/NR3 sent
Aston Ambulatory Care Center			
Children's Medical Center of Dallas			
Dallas County Mental Health			
General Clinical Research Center			
Moncrief Cancer Center/Fort Worth			
Parkland Health & Hospital System			
Presbyterian Hospital of Dallas			
Sprague Clinical Sciences Center			
St. Paul Medical Center			
Texas Scottish Rite Hospital for Children		XX	

Veteran's Affairs Medical Center				
Zale Lipshy University Hospital	xx			
Other (specify below)				

Other approvals needed:

	Environmental Health & Safety Committee
	Radiation Safety Committee
	IRB at the Veteran's Affairs Medical Center
	IRB at Presbyterian Hospital of Dallas
	Grants Management (UT Southwestern)
	General Clinical Research Center
XX	Form NR2/NR3
	Other (specify below)

Have all approvals been requested?

XX	Yes
	no (explain below)

8. OTHER PAPERWORK REQUIRED:

a) Project summary including any questionnaires, surveys, telephone scripts, etc.

Also, when applicable:

b) Complete grant application, with budget (when project is federally funded). Block out confidential salary information and total dollar amount.

c) Consent form, information sheet, brochure, and/or letter, script for verbal consent.

d) Recruitment materials (e.g., posted notices, advertisements, telephone script, letters, etc.)

COMMENTS:

SOUTHWESTERN

THE UNIVERSITY OF TEXAS
SOUTHWESTERN MEDICAL CENTER
AT DALLAS

Institutional Review Board

TO: Phillipe Zimmern, MD
c/o Allison Ahrens, RN
Urology - 9110

FROM: For: Ronald Ramus, MD
Institutional Review Board 4 – Chairperson
IRB - 8843

DATE: 02 April 2004

SUBJECT: **Continuing IRB Review – Expedited Approval**
IRB File Number: 0402-222
Project Title: Correlation Between the Biomedical and Histochemical Properties of the Human Anterior Vaginal Wall

The Institutional Review Board reviewed this research activity on an expedited basis. Your protocol was approved for continuation for the period beginning 16 April 2004 and expiring on 15 April 2005. Your HIPAA Waiver was also approved. The Board waived the use of a consent form in accordance with 45 CFR 46.116(d).

Please report to the IRB any unexpected or serious adverse events that occur during the study. Any proposed changes in this research must be submitted to the IRB for review and approval prior to implementation, except for immediate changes necessary to assure research subject safety, which must be reported to the IRB within two days.

This study will require continuing review from the IRB and a reminder will be mailed to you 60 days prior to the **expiration date of 15 April 2005.**

Should you have any questions, please telephone Reda Hall in the IRB office at 214.648.3378.

RR/mh

APPENDIX B

LIGHT MICROSCOPY AUTOMATED TISSUE PROCESSING SCHEDULE

Table A Light microscopy automated Tissue processing schedule, Shandon Hypercenter XP

	Reagent Process	Time (Minutes)
1	70% alcohol	60
2	80% alcohol	60
3	95% alcohol in 4% phenol	60
4	absolute alcohol	90
5	absolute alcohol	90
6	absolute alcohol	90
7	absolute alcohol	90
8	alcohol/chloroform(1:1)	90
9	Chloroform	60
10	Chloroform	90
11	Paraffin wax	120 @ 60^{o}C
12	Paraffin wax	120 @ 60^{o}C

The paraffin blocks obtained from the machine are stored until ready for analysis.

APPENDIX C

HEMATOXYLIN AND EOSIN STAINING PROTOCOL

Reagents: STF

Meyer's Hematoxylin solution

Eosin 1% aqueous or 0.5% alcoholic solution

Ammonia water pH= 8

Distilled water 1000 ml + 2-3 ml ammonium peroxide

Procedure:

1. If the tissue sample is preserved in paraffin wax, deparaffinize and hydrate the section to water.

2. Wash the section in tap water for 5 minutes.

3. Stain in Mayer's Hematoxylin solution for 5 minutes.

4. Rinse in tap water

5. Treat with ammonia water until section turns blue in color.

6. Rinse in water and observe section in microscope. Nuclei should be blue in color with negligible background stain. Repeat steps 4-7 if necessary.

7. Wash in water for 10 minutes

8. Place in aqueous eosin or dehydrate through graded alcohol to 95% before placing in alcoholic eosin for 5 minutes

9. Sections in aqueous eosin should be quickly rinsed in water and then dehydrated through graded alcohol to xylene (3 changes) and mounted.

10. Sections stained in alcoholic eosin should be washed in 3 changes of 100 % alcohol, cleared in xylene and mounted in a synthetic mount.

APPENDIX D

LEICA EM AUTOMATIC TISSUE PROCESSING

Table B Two step program: Program 1

Program 1:		
	Reagent Process	Time(Minutes)
1	Buffer Wash	5
2	Buffer Wash	5
3	Osmium tetroxide	60
4	Distilled water	5
5	Distilled water	5
6	50% alcohol	10
7	70% alcohol	10
8	95% alcohol	10
9	Ethyl Alcohol	10
10	Ethyl Alcohol	20
11	Ethyl Alcohol	20
12	Ethyl Alcohol	10
13	Propylene Oxide	5
14	Propylene Oxide	5
15	Propylene oxide/Resin	2:130minutes

Table C Two step program: Program 2

Program 2:		
	Reagent Process	Time(Minutes)
1	Propylene oxide	1:160 minutes
2	Propylene oxide	2:160 minutes
3	Resin	90
4	Resin	90

APPENDIX E

EM STAINING PROTOCOL

Reagents:

Reynold's Lead Citrate

Dissolve 1.33 gm Lead Nitrate in 30 ml double distilled water that has been boiled to remove the CO2. Then dissolve 1.76 gm of Sodium Citrate in above mix. Shake well for 1 minute at 5-minute intervals over a period of 30 minutes. Add 1N(++:>+) Sodium Hydroxide drop by drop till the solution turns just clear. The suspension is diluted with distilled water and mixed by inversion. Filter before use.

Uranyl Acetate:

Make a super saturated solution of Uranyl Acetate in 50 % Ethyl alcohol and place in oven overnight at 60o C. Remove, cool and double filter. Store in dark bottle in dark until required. Filter before use suing a swinex filter.

Procedure:

1. Float grids on a drop of Uranyl acetate on a dental wax sheet in a Petri dish in the dark for 5 minutes.
2. Rinse grids in 50% alcohol (20-30 dips) and repeat using double distilled water and blot dry with a clean dry filter paper.
3. Float grids on Reynold's Lead citrate for 5 minutes in a petri dish containing NaOH pellets.
4. Rinse grids in double distilled water containing 2 drops of 1N NaOH and repeat suing double distilled water. Blot dry on filter paper.

APPENDIX F

BIOMECHANICAL TESTING DATA

Table 1 Group 1 data points

UTS	YP	E	Pre-transition strain	Age	Tissue thickness
1.6597	0.5676	6.9	0.0817	76	3.81
0.2875	0.6479	0.55	0.0876	72	4
0.3304	0.1296	3.84	0.0016	68	1.93
2.2886	0.4877	5.65	-0.0386	53	2.24
0.8621	0.7786	1.5	0.1387	80	4.93
0.821	0.4317	2.5	0.0196	69	2.65
1.6775	0.4337	5.21	0.0344	69	4.92
1.722	0.5389	5.8	-0.0026	66	2.52
1.9675	0.4345	5.7	0.0093	60	2.11
2.5599	0.3092	12	0.0071	53	1.95
1.1137	0.3927	1.67	0.0351	55	4.22
2.5375	0.724	5.28	-0.064	79	2.01
1.1761	0.5501	4.84	0.0447	81	3.97
1.2286	0.4046	3.5	-0.0263	68	2.7
1.8165	0.305	1.79	0.0155	74	2.35
0.8083	0.3096	3.1	-0.0299	79	5.15

Table 2 Group 2 data points

UTS	YP	E	Pre-transition strain	Age	Tissue thickness
1.0833	0.714	1.9	0.2073	70	2.86
3.2514	0.6443	5.25	0.0894	52	2.16
2.1537	0.2516	9.8	0.007	81	2.21
1.3924	0.3563	3.3	-0.0158	75	3.36
2.4535	0.2634	13.15	0.023	77	2.22
4.7736	0.5181	15.17012	0.1755	72	1.4
1.96	0.2798	9.478421	-0.0185	60	1.42
4.2172	0.2779	21.0599	0.031	82	1.47
3.3369	0.506	9.568367	0.1256	59	1.45
2.1195	0.2976	7.203155	-0.0214	63	1.64
1.5453	0.1627	9.19122	0.005	77	1.59
1.0076	0.0553	11.55337	-0.046	82	2.24
1.9118	0.308	9.126235	0.1191	61	1.71
2.098	0.1951	11.2805	4.1821	71	2.22
0.9506	0.1503	4.775707	0.1205	56	2.14
2.6725	0.438	6.489132	0.0307	58	2.15

Table 2-*Continued*

1.2343	0.3778	3.926888	-0.0177	57	2.36
1.7284	0.3891	6.371702	0.0386	75	2.06
1.1231	0.2432	4.543988	0.0045	58	1.63
1.889	0.4158	5.662046	0.0061	74	2.22
0.391	0.2843	1.725699	-0.0094	83	5.07
2.7693	0.1577	16.00293	-0.0147	74	1.68
1.8171	0.3203	7.5974	0.0612	85	2.47

Table 3 Control sample data

UTS	YP	E	Pre-transition strain	Age	Tissue thickness
1.8116	0.1876	13.07981	0.0209	75	2.35
1.3094	0.085	11.71676	-0.0094	58	2.96
1.0037	0.1149	5.826353	-0.003	83	3

APPENDIX G

LM DATA

Table 1 Thickness of the epithelium in the unstretched and stretched prolapse sample

	Unstretched prolapse tissue(μm)	Stretched prolapse tissue (μm)
1	70.29	27.5
2	66.94	29.62
3	66.76	24.31
4	72.18	25.37
5	77.39	24.34
6	80.73	30.66
7	66.08	28.56
8	77.17	24.31
9	73.91	27.48
10	67.67	37.01
11	68.56	31.73
12	68.56	35.94
13	65.51	32.77
14	78.48	31.71
15	76.14	35.03
16	69.25	27.48
17	71.35	34.9
18	70.41	34.9
19	75.58	32.77
20	77.7	34.24
Average	72.033	30.5315
Std Dev	4.736032	4.174889

APPENDIX H

HISTOMORPHOMETRY MEASUREMENTS

Table 1 EM measurement data showing periodicity and diameter of the collagen fibers in the control and prolapse sample.

Periodicity – Control unstretched	Periodicity – Control stretched	Periodicity – Prolapse unstretched	Periodicity –Prolapse stretched		Diameter-Control unstretched	Diameter-Control stretched	Diameter-Prolapse unstretched	Diameter-Prolapse stretched
56.46	55.57	59.45	67.27		63.01	62.05	60.30	54.77
50.52	48.51	57.26	58.33		66.04	58.87	59.08	52.20
52.33	47.66	65.57	66.48		65.05	60.22	52.69	64.90
52.74	50.03	62.48	68.93		66.58	58.87	61.47	66.93
52.40	53.89	48.29	63.98		68.60	54.41	56.79	70.95
49.62	51.14	60.03	69.08		67.40	55.22	54.75	55.35
51.84	50.52	58.08	61.02		62.87	57.27	60.50	66.66
49.34	55.80	62.95	63.80		62.87	57.57	57.80	62.36
50.74	52.03	62.95	66.08		60.03	53.32	60.50	59.29
51.52	50.03	52.88	63.40		52.91	51.84	47.59	54.77
49.31	52.33	61.70	60.33		53.58	53.45	47.15	64.14
56.46	53.89	47.87	56.79		63.60	51.84	51.17	61.34
50.14	56.73	52.88	63.40		62.87	56.47	70.88	60.81
48.29	48.87	55.89	71.99		65.05	61.37	60.50	66.71
46.44	54.69	57.91	72.75		64.40	59.70	61.47	55.35
49.75	56.27	56.27	68.46		61.70	52.01	58.92	58.33
55.08	52.01	56.48	66.08		63.78	51.84	62.01	52.71
51.52	51.74	60.83	69.04		60.03	53.25	66.54	68.84
48.58	54.69	65.86	69.96		60.05	60.46	67.91	61.34
48.58	52.93	62.30	58.25		64.40	60.22	59.00	58.33
54.34	52.74	66.13	69.94		60.28	58.15	56.63	54.70
52.74	54.41	60.49	64.34		63.01	59.87	54.39	56.91
48.29	54.52	59.87	58.90		60.72	53.32	54.39	55.56
51.44	49.55	63.38	61.65		66.44	53.32	52.88	58.33
50.74	49.55	61.40	58.31		67.87	53.23	64.75	58.27

Table 1-*Continued*

54.34	56.00	61.66	66.38		62.93	54.84	58.44	62.68
53.56	49.75	48.77	65.45		57.15	66.31	60.27	70.37
52.88	54.41	69.79	63.11		60.72	46.80	55.23	64.90
45.41	52.72	61.78	69.94		61.48	56.47	60.68	57.34
55.73	52.74	68.12	71.10		57.88	50.10	60.95	60.24
55.73	52.81	54.69	68.06		67.34	64.54	62.24	68.18
44.41	56.27	64.47	66.05		47.95	61.31	47.97	61.84
48.69	59.30	58.18	69.55		60.72	63.09	66.92	67.12
53.68	54.52	60.69	66.69		64.30	67.74	61.59	68.46
42.98	56.48	63.67	73.50		65.05	66.13	43.99	64.84
45.18	51.52	62.20	59.53		65.86	69.37	58.53	63.50
43.16	53.10	71.61	65.45		64.87	53.25	72.09	67.10
46.98	50.16	53.39	72.00		63.62	51.71	71.61	67.33
39.55	55.15	65.23	62.48		63.42	56.82	68.12	71.56
44.76	50.16	65.68	51.19		56.48	58.27	61.25	64.60
47.92	58.30	63.27	57.42		57.88	71.09	59.28	58.07
55.91	54.52	55.77	64.58		61.37	64.11	75.55	49.37
48.90	58.58	65.36	63.11		63.62	64.11	68.62	60.92
43.01	59.13	62.80	61.00		59.13	56.00	56.66	59.10
44.30	56.27	62.50	60.22		64.40	60.64	44.50	54.23
54.31	56.48	58.70	58.75		63.01	57.55	54.05	57.07
49.31	54.34	60.45	65.39		56.88	62.99	48.06	56.66
49.21	49.55	60.02	65.91		62.14	59.45	58.61	58.07
50.52	54.31	63.27	68.15		66.73	56.84	54.31	54.44
52.74	51.12	64.05	64.44		63.42	56.30	63.03	52.32
52.01	51.12	67.16	68.15		58.15	50.61	69.59	55.63
46.66	52.72	60.68	62.33		58.91	54.42	49.34	56.70
52.40	57.51	64.34	65.97		65.86	57.96	65.16	64.68

Table 1-*Continued*

55.01	54.34	59.39	62.21		62.63	52.93	72.99	62.23
52.33	55.93	64.05	72.09		62.22	57.55	50.52	68.82
55.38	51.12	65.15	68.79		52.40	52.93	72.33	65.39
49.31	57.60	62.80	67.59		66.48	57.96	57.26	61.19
42.17	54.90	61.60	67.98		66.48	61.03	70.31	61.36
47.50	56.48	60.27	65.39		62.95	52.52	57.91	63.46
53.39	53.89	63.80	68.79		63.42	54.47	66.65	70.40
53.34	54.59	58.55	61.14		79.41	52.93	57.71	58.36
46.22	49.55	62.02	59.64		79.97	52.93	49.91	60.84
47.57	55.91	60.27	64.69		79.41	52.16	67.11	84.13
51.01	55.93	64.75	64.39		79.82	54.72	65.18	54.18
42.07	54.64	67.16	63.60		75.36	51.18	67.96	53.71
48.74	55.45	64.05	66.75		78.14	51.35	67.77	56.52
45.55	55.80	56.78	63.19		77.20	50.88	54.64	53.71
44.32	55.57	58.36	68.24		78.93	51.87	63.30	62.89
51.11	57.73	64.98	64.16		73.64	55.62	66.73	67.81
47.57	57.35	64.98	69.59		79.11	51.18	55.91	65.16
52.91	55.08	65.39	72.08		78.14	50.88	55.38	65.62
46.80	49.00	60.00	66.19		84.72	56.97	56.66	63.99
37.41	50.51	62.42	61.66		86.95	56.90	58.08	71.73
51.01	50.03	68.98	64.16		74.48	51.40	54.97	64.79
45.38	48.50	65.41	65.73		68.68	50.35	62.48	62.09
53.56	60.62	61.65	70.14		70.46	55.91	65.03	63.85
53.37	52.88	61.65	57.60		71.21	56.90	63.62	57.52
56.09	52.03	59.49	68.71		74.79	56.43	62.63	50.72
54.23	52.69	59.29	67.34		73.34	56.00	63.36	62.09
41.36	52.33	63.98	66.65		78.93	51.57	63.77	58.13
54.82	52.54	64.90	49.53		77.92	57.88	68.64	59.83

Table 1-*Continued*

51.31	58.15	68.18	56.54		62.62	59.45	63.71	52.34
54.82	53.55	65.94	45.76		67.62	55.21	65.29	52.07
51.11	49.93	64.36	62.10		78.50	50.00	71.81	54.23
50.07	51.74	62.50	54.40		80.27	51.87	61.03	52.07
55.63	51.14	62.97	59.48		72.65	53.39	60.84	61.85
51.11	47.66	66.07	61.62		66.93	52.93	59.00	56.84
51.31	54.24	60.07	56.54		67.01	49.77	64.01	53.03
44.32	56.18	60.66	56.54		68.23	53.41	56.30	54.99
60.58	48.66	59.10	62.70		63.42	51.57	60.70	65.29
49.37	51.04	55.73	55.92		69.06	55.82	73.52	65.92
55.54	62.38	55.36	64.73		66.15	55.82	64.19	61.62
55.14	68.24	53.39	63.60		70.98	57.52	63.71	63.60
50.07	61.66	54.27	67.62		74.48	58.42	59.26	63.05
53.85	58.30	56.52	63.17		74.18	59.09	51.84	67.77
44.90	52.33	55.64	57.97		72.63	59.09	68.64	66.15
47.13	55.15	55.36	56.84		69.04	56.90	61.03	63.28
52.18	47.87	55.45	49.19		65.60	62.99	69.13	66.62
49.78	58.74	53.20	65.03		64.73	63.95	76.70	66.62
54.70	55.08	55.36	65.58		69.65	53.39	53.88	66.09
49.76	56.66	68.71	56.84		67.14	70.23	57.96	62.87
52.49	55.80	55.93	59.83		65.60	73.32	53.03	52.91
55.63	52.55	52.72	63.03		81.15	75.77	60.19	52.88
52.18	55.80	55.91	55.04		64.25	63.28	50.78	58.15
57.78	57.73	46.35	65.03		75.00	61.11	60.95	47.41
54.77	53.58	52.74	58.67		75.06	59.03	54.79	51.84
57.33	56.12	59.13	59.68		74.74	67.01	55.28	57.60
51.61	53.58	52.74	66.69		70.23	70.04	60.09	59.88
50.19	53.70	67.40	61.62		67.62	67.33	64.19	57.88

Table 1-*Continued*

56.79	60.83	56.00	66.29		76.26	68.68	62.02	57.20
53.34	58.65	57.60	71.77		70.23	69.80	55.71	67.41
57.78	56.48	51.14	64.01		71.99	66.21	54.47	59.81
58.27	55.73	60.79	57.09		64.81	64.81	52.57	54.41
51.61	58.50	57.53	58.43		76.45	67.83	57.01	60.39
56.64	59.96	56.48	59.83		78.15	64.81	55.18	59.13
55.19	52.40	54.90	65.28		72.66	65.11	57.70	56.66
56.64	55.64	56.00	59.29		72.12	60.20	62.43	59.96
56.64	55.91	59.19	59.66		71.61	58.52	63.09	61.37
54.51	55.64	54.52	66.29		68.33	54.87	63.21	58.08
58.77	55.89	56.12	64.73		68.33	57.97	58.74	59.13
56.64	54.64	56.48	65.58		70.59	68.40	57.26	60.79
59.49	55.91	54.34	67.14		73.40	67.01	58.74	54.52
56.84	52.74	60.72	66.29		72.47	69.06	73.86	53.56
56.84	54.52	60.72	65.41		69.87	64.03	65.03	54.90
56.66	55.73	59.11	66.25		72.66	67.83	52.88	62.48
55.19	52.16	59.30	65.88		70.26	64.25	51.44	57.53
54.77	54.64	62.63	60.92		74.08	68.23	56.73	62.38
52.71	55.38	49.62	71.83		75.93	68.81	62.22	67.57
53.05	54.05	55.93	68.01		74.70	63.36	59.64	64.08
56.27	53.70	57.86	67.99		77.34	62.04	57.91	62.32
53.27	55.89	55.36	71.40		76.60	59.31	63.20	58.30
55.26	58.59	62.38	68.01		74.70	67.16	58.59	64.08
55.74	55.01	64.39	59.64		76.94	65.97	54.05	56.12
52.86	56.48	59.81	65.78		70.40	66.29	55.89	61.70
54.23	55.89	59.43	72.03		73.87	66.29	66.50	63.20
53.87	55.89	58.93	58.07		73.87	68.25	63.62	60.72
48.10	56.27	59.45	61.84		75.12	65.62	52.23	57.35

Table 1-*Continued*

53.87	54.34	63.36	60.33		68.33	65.94	60.05	64.61
55.97	56.27	63.36	63.15		80.46	67.60	60.13	63.30
48.74	56.73	60.13	66.94		76.00	66.93	67.19	57.86
55.33	56.46	61.37	66.79		77.09	63.05	75.77	70.26
52.86	54.31	62.87	56.07		79.61	68.30	73.59	69.36
49.37	55.01	60.83	59.64		71.83	67.77	77.16	61.62
56.66	60.83	66.58	67.11		78.39	66.93	69.30	55.94
51.61	55.01	56.48	56.00		75.64	69.06	72.92	59.64
55.91	55.08	63.62	68.76		76.34	66.29	64.40	70.85
56.27	58.08	61.66	73.50		77.19	64.01	64.87	67.94
49.16	58.08	62.22	70.45		78.20	64.71	65.67	60.87
54.51	55.73	65.18	72.33		72.56	67.18	68.99	63.68
49.03	53.58	62.03	74.33		74.82	61.85	61.66	68.98
54.86	58.08	62.14	65.98		72.89	64.71	66.73	63.23
54.23	55.91	59.96	63.19		74.57	62.70	67.81	63.64
46.67	54.05	71.17	74.59		76.13	69.88	62.38	59.31
48.66	55.91	61.04	82.14		73.39	65.46	68.76	67.72
47.65	54.05	63.26	47.50		75.34	61.11	70.96	66.02
52.86	55.38	61.04	63.30		73.16	66.87	73.15	64.64
49.76	53.70	65.67	60.83		74.82	62.70	78.08	59.07
49.37	58.15	56.27	65.81		74.79	65.11	57.71	64.43
53.05	51.44	61.66	69.36		68.33	61.87	69.36	60.56
54.77	55.18	63.62	55.15		71.40	67.77	71.24	64.07
44.76	56.46	60.39	68.02		73.40	66.93	71.24	70.97
52.74	52.74	59.45	65.86		72.03	64.03	62.93	73.11
47.95	56.66	57.88	62.65		75.34	66.46	58.74	77.09
51.14	57.60	62.38	80.72		72.13	64.67	76.29	75.80
48.58	56.27	65.57	62.67		76.99	67.01	66.44	74.15

Table 1-*Continued*

51.34	52.91	59.81	49.98		65.72	69.80	57.26	77.41
49.75	56.48	62.38	65.52		65.70	62.70	65.05	81.60
49.75	52.91	60.83	42.07		65.72	62.89	61.45	76.02
49.75	57.26	62.14	52.06		75.39	63.28	57.15	64.14
49.62	50.14	61.16	68.40		73.79	63.34	50.14	67.63
49.75	50.14	62.14	50.58		78.52	61.22	60.62	75.52
47.95	55.80	58.61	47.29		77.07	66.87	61.45	72.03
49.55	60.03	57.08	57.70		75.32	62.70	70.31	70.98
51.22	58.74	57.60	58.55		75.11	66.87	64.61	73.53
49.52	56.66	60.22	63.63		76.18	63.28	59.30	74.00
47.92	53.70	58.74	60.03		77.74	64.03	70.31	74.08
49.75	55.80	60.22	61.96		77.35	63.42	68.24	72.52
51.74	58.74	62.30	50.61		72.68	66.15	63.62	71.13
48.58	56.46	57.91	62.02		78.67	63.76	55.73	72.42
50.44	52.16	55.57	69.92		72.75	67.33	75.35	77.09
49.52	55.73	57.73	62.10		79.56	62.89	72.33	69.79
46.52	54.05	57.73	67.65		74.57	62.56	73.01	84.35
51.14	55.57	58.15	61.18		77.52	59.11	64.87	75.27
49.62	55.18	60.13	44.32		75.11	62.70	65.50	73.17
52.93	55.73	58.58	46.67		72.47	66.29	69.36	76.26
50.32	57.15	55.73	50.93		76.01	61.54	68.62	66.67
48.10	55.01	65.73	52.91		71.97	69.06	65.67	82.55
49.68	57.91	55.57	58.05		77.54	64.81	72.75	76.34
51.31	59.30	68.97	50.19		76.40	64.81	67.05	71.71
48.10	61.48	57.60	50.60		76.69	65.68	69.59	80.83
52.86	54.34	57.20	47.65		76.40	59.75	66.73	70.27
47.46	55.01	61.23	46.25		73.24	59.11	62.77	78.41
51.90	55.80	63.24	47.65		74.82	59.75	61.04	75.87

Table 1-*Continued*

51.90	55.80	64.42	56.66		73.87	66.29	59.19	62.25
50.32	50.77	62.68	55.63		73.99	64.81	68.86	85.26
50.32	52.23	62.68	52.86		73.73	63.34	62.48	80.47
48.74	51.52	64.28	49.76		70.53	65.44	67.77	76.26
51.51	52.33	61.23	55.74		67.33	64.01	67.77	83.33
49.78	56.48	64.42	54.86		73.52	61.22	64.40	74.75
46.58	58.65	61.02	57.89		72.02	62.70	59.36	71.71
Average	Average	Average	Average		Average	Average	Average	Average
51.19	54.71	60.37	62.61		70.23	60.71	62.11	63.76
Std dev	Std dev	Std dev	Std dev		Std dev	Std dev	Std dev	
3.953068	3.088221	4.40	6.86		6.798515	5.918643	6.90	7.71

REFERENCES

1. Subak, L L, Waetjen, L E, Eeden S, Thom D H, Vittinghoff E, Brown J S, Cost of pelvic organ prolapse surgery in the United States, Obstetrics & Gynecology 2001; 98:646-651.

2. Weber, A M, Walters, M D, Anterior vaginal prolpase: Review of anatomy and techniques of surgical repair, Obstet Gynecol 1997; 89:311-8.

3. Weber, A.M, Buchsbaum G.M, Chen, B, Clark A L, DamaserM,S, Daneshgari,F,et al, Basic Science and Translational Research on Female Pelvic floor Disorders:Proceedings of an NIH-Sponsored Meeting. Neurology and Urodynamics 23:288-301(2004).

4. Siddique S A, Vaginal anatomy and physiology, Journal of pelvic medicine and surgery, 2003; 9; 263-272.

5. Ridder DD, The use of biomaterials in reconstructive urology, European Urology Supplements 1 (2002)7-11.

6. Cosson, M M, Debodinance ,P, Boukerrou M, Chauvet, M P, Lobry, P, Crepin G, et al. Mechanical properties of synthetic implants used in the repair of prolapse and urinary incotinence in women: which is the ideal material?, Int Urogynecol J,(2003)14:169-178.

7. Krause, H, Goh, J, Khoo,S K, Williams, R, Galloway, S, Biocompatible properties of surgical mesh using an animal model. ICS nad IUGA.

8. Chuong C J, Sacks,M S, Johnson Jr R L, Reynolds, R, On the anisotropy of the canine diaphragmatic central tensdon, J. Biomechanics, Vol 24,No 7,pp.563-576,1991.

9.Young B, Heath J W, Wheater's functional histology –A text and color atlas.5th ed. Churchill Livingstone; 2001.

10.Bancroft J D, Stevens A, Theory and practice of histological techniques, 4th ed. Churchill Livingstone.

11. Kushner,L, Mathrubutham, M, Burney, T, Greenwald, R, Badlani, G, Excretion of collagen derived peptides is increased in women with stress urinary incontinence, Neurourol. Urodynam. 23:198-203,2004.

12. Fung YC. Biomechanics. Mechanical properties of living tissues.2nd ed. New York: Springer;1993.

13. Ettema, G.J.C, Goh, J.T.W., Forwood M.R, A new method to measure elastic properties of plastic- viscoelastic connective tissue, Medical Engineering and Physics 20 (1998) 308-314.

14. Ottani, V. Raspanti, M, Ruggeri,A, Collagen structure and functional implications, Micron 32(2001) 251-260.

15. Ratner BD, Hoffman A S, Schoen F J, Lemons JE. Biomaterials science, An introduction to materials in medicine. 2nd ed. Elsevier academic press; 2004.

16. http://www.obgyn.net/displayarticle.asp? page=/women/articles/miklos-amb_procedures)

17. http://www.nlm.nih.gov/medlineplus/ency/imagepages/9064.htm)

BIOGRAPHICAL INFORMATION

Aradhana Bhatt completed her Bachelor of Science in Electrical and Electronics from Manipal Institute of Technology, Manipal, Karnataka, India in June 2002. She joined for the Masters program at the joint program of Biomedical Engineering program at University of Texas at Arlington/ University of Texas Southwestern Medical center in August 2003. During the course of her education she worked on various class projects. She worked as a Graduate Teaching assistant at the Department of Biomedical engineering for two semesters. The opportunity to work on this project was a unique experience in understanding the anisotropic nature of living tissues. The outcome of this study could help in understanding the pathophysiology of the pelvic floor disorders. In the future she looks forward to pursue a career in the Biotechnology field and eventually pursue a Doctorate in Philosophy.